The Electronic Structure of Methylene[1a]

James F. Harrison[1b] and Leland C. Allen

Contribution from the Department of Chemistry, Princeton University, Princeton, New Jersey 08540. *Received September 11, 1968*

Abstract: *Ab initio* valence-bond wave functions are reported for the $^3B_1$, $^1A_1$, and $^1B_1$ states of CH_2 as a function of angle with R(C–H) = 2.00 bohrs. Up to 48 valence-bond structures for each state were used to expand the variational wave functions (each VB structure is a single term of an expansion which is composed of those appropriate linear combinations of determinants required to assure a definite spin and space symmetry). A nonorthogonal free atom basis constructed with Gaussian lobe functions was employed. Calculations with scaled hydrogen orbitals were likewise carried out. The total energy of the ground state, $^3B_1$, near its equilibrium position is E_T (140°) = −38.9151 Hartree units. *Ab initio* MO–SCF wave functions were also computed as a function of angle for the $^1A_1$ state, and MO wave functions for the $^{1,3}B_1$ states were constructed from single excitations of the MO $^1A_1$ state. The order of states is computed to be $^3B_1 < {}^1A_1 < {}^1B_1$ with large equilibrium angle for $^{1,3}B_1$, 108° for $^1A_1$, and an $^1A_1$–$^1B_1$ energy separation of 1.52 eV. Spectroscopic data are available for these properties, and the agreement between theory and experiment is quite good. Larmor diamagnetic susceptibility terms are computed to be -19.75×10^{-6} and -19.57×10^{-6} erg/(G² mole) for the $^1A_1$ and $^1B_1$ states, respectively, compared to an estimated experimental value of -12×10^{-6}. The $^3B_1$ heat of atomization is calculated as 6.36 eV (experimental value $\cong$ 8.5 eV). Expectation values of the following quantities (for which experiments are currently lacking) have been obtained as a function of angle: dipole moments, quadrupole tensor, diamagnetic contribution to the nuclear magnetic shielding constant of the protons, diamagnetic anisotropy, electric field gradient tensor, quadrupole coupling constants for deuterated methylene, $\langle 1/r_H \rangle$, $\langle 1/r_C \rangle$, heats of atomization of the $^1A_1$ and $^1B_1$ states, the $^3B_1$–$^1A_1$ energy separation, and oscillator strength for singlet–singlet transitions. Considerable attention has been given to detailed descriptions of the charge distributions and to the implications of our results for divalent carbon chemistry. There is a long and intricate history of experimental and theoretical attempts to elucidate the electronic structure of methylene, and in order to aid over-all understanding of this molecule, a rather extensive review and analysis of previous work has been included.

I. Introduction

Methylene is the basic unit for divalent carbon chemistry and is one of the most important molecules in chemistry. The existence of a triplet ground state and relatively low-lying excited singlet state in CH_2 has led to a unique and rapidly developing branch of organic chemistry. It is challenging, and perhaps surprising, that spectroscopic experiments on this comparatively simple species have been very difficult and often ambiguous. Similarly, there has been a long sustained and rather unsuccessful history of theoretical effort.

The theoretical electronic structure study presented here is an *ab initio* valence-bond treatment of methylene's ground and low-lying excited states. For constructing various spin states in an eight-electron, three-center system such as CH_2, the valence-bond approach is particularly suitable for generating high accuracy, chemically interpretable wave functions. For comparison, an *ab initio* self-consistent field molecular orbital solution was also obtained for one of the states. In view of the history and importance of this species, it is satisfying that the present study is in general agreement with the best existing experimental work and that experimental and theoretical results now may be treated with roughly equal confidence. A variety of other properties, not presently available experimentally, also has been predicted.

In the next section the wave-function formulation and basis set determination is given. Section III presents, and compares with experiment, results on the order of states, geometries, binding energies, and transition probabilities. Section IV predicts some one-electron properties, most of which have not been obtained experimentally. Section V is an extensive review and analysis of prior theoretical work and a brief outline of the experimental situation. Taken together with a review by Gaspar and Hammond[2] this provides the background which, because of its rich and intricate history, is particularly necessary and appropriate to an understanding of methylene.

II. Method of Calculation

A. Description of Technique. Most of the energy calculations carried out in this study have employed the valence-bond (VB) formalism taking into account fully the nonorthogonality of the atomic basis. This was accomplished by using the Löwdin formulation[3] for performing linear variational calculations over a basis of Slater determinants, the elements of which are nonorthogonal. A digital computer program for this procedure has been written by Erdahl.[4] The program is capable of solving the linear variational problem over a basis of 80 valence-bond structures each of which may be a linear combination of eight Slater determinants (each determinant in turn consisting of up to 32 spin orbitals). We have occasion to compare the results of a valence-bond calculation with an LCAO–MO calculation over the same basis. The MO results have

(1) (a) This research was supported in part by the Chemistry Section of the National Science Foundation, Grant No. NSF-GP-8907, and the Directorate of Chemical Sciences of the Air Force Office of Scientific Research, Contract No. AF 49(638)-1625. (b) Author to whom inquiries should be addressed at Department of Chemistry, Michgan State University, East Lansing, Mich. 48823.

(2) P. P. Gaspar and G. S. Hammond, "Carbene Chemistry," W. Kirmse, Ed., Academic Press, New York, N. Y., 1964, pp 235–274.
(3) P. O. Löwdin, *Phys. Rev.*, 97, 1474, 1490, 1509 (1955).
(4) R. M. Erdahl, Ph.D. Thesis, Princeton University, 1966.

Table I. Atomic Basis and Primary Structures Used in Constructing VB—Doubly Occupied 1s and 2s

Atomic basis	Primary structures
1. Carbon 1s	1) 1 2 3 4
2. Carbon 2s	2) 1 2 3 5
3. Hydrogen 1 1s + hydrogen 2 1s	3) 1 2 3 6
4. Carbon p_z	4) 1 2 3 7
5. Hydrogen 1 1s − hydrogen 2 1s	5) 1 2 4 5
6. Carbon p_x	6) 1 2 4 6
7. Carbon p_y	7) 1 2 4 7
	8) 1 2 5 6
	9) 1 2 5 7
	10) 1 2 6 7

been obtained *via* the Hartree–Fock–Roothaan equations. All integrals were generated over Gaussian lobe functions and then transformed to the basis being used in the calculation. For example, in carrying out a VB calculation over an atomic orbital basis, the integrals were evaluated over the Gaussians and then transformed into the atomic orbital basis.[5] The atomic orbitals are close to atomic Hartree–Fock solutions. The notation used for the Slater determinant has been described previously[4] and will only be briefly outlined here. We restrict ourselves to systems containing an even number of electrons and consider only determinants having the number of α spins equal to the number of β spins. This requires that we consider the $S_z = 0$ component of triplets, etc. We collect all of the spatial orbitals associated with the same spin and call this ordered set of spatial orbitals a primary structure. Each determinant requires for its definition two primary structures, one to define the α-spin configuration and one to define the β-spin configuration. A linear combination of determinants which is an eigenfunction of the spin operator and is of definite spatial symmetry is called a valence-bond structure. The linear variation problem is then solved over a basis of valence-bond structures.

B. **Basis Functions.** We use the full nonrelativistic Hamiltonian in atomic units

$$H = \sum_{i=1}^{8}\left(-{}^1/_2\nabla_i^2 - \sum_{\mu=1}^{3}\frac{Z_\mu}{r_{\mu i}}\right) + \sum_{i>j}^{8} 1/r_{ij} + \sum_{\mu>\nu}^{3}\frac{Z_\mu Z_\nu}{R_{\mu\nu}}$$

and we introduce the atomic basis presented in Table I. In C_{2v} the functions 1, 2, 3, and 6 transform as a_1, 4 and 5 as b_2, and 7 as b_1. We take the x axis as the C_2 axis so that in the linear configuration the z axis is the internuclear line (see Figure 1). Throughout this study we take the CH distance as 2.00 bohrs.

C. **Valence-Bond Considerations.** We have carried out three series of calculations employing the VB formalism.

(a) VB I. In the first VB calculation we consider only determinants having the carbon configuration $(1s)^2(2s)^2$; *i.e.*, we do not allow for hybridization of the carbon 2s and 2p orbitals. Under these conditions there are of the eight electrons in the problem only four "active." The number of primary structures which arise from the permutation of these four electrons among the atomic orbitals 3 through 7 is $\binom{5}{2} = 10$, and from these 10 primary structures (shown in Table I) we may form 100 unique 8 × 8 determinants. We then use projection operators to project the space spanned by these determinants into singlet and triplet subspaces. Then within the singlet and triplet spaces we project out all functions of symmetry A_1, B_1, and B_2. The VB structures so generated are displayed in Table II. The linear variational problem was solved within each space of definite symmetry and spin. The potential curves which were generated are shown in Figure 2. The energies used to construct these curves are listed in Table III. The wave functions are not presented but are available upon request. We note that all states correlate with the proper linear symmetry, and we present in Table IV the energies of the various states of linear CH_2 relative to the $^3\Sigma_g^-$ state. Since we have employed only valence-state orbitals, the states with rather high energies have little physical meaning.

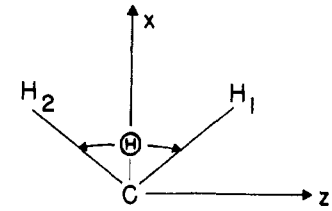

Figure 1. Coordinate system.

(b) VB II. In the second calculation we consider those determinants having the carbon configuration $(1s)^2$; *i.e.*, we allow completely for hybridization between the carbon 2s and 2p. Under these conditions there are six "active" electrons which may be permuted among the six spatial orbitals 2 through 7. This gives rise to $\binom{6}{3} = 20$ primary structures (see Table V) from which we may form 400 8 × 8 determinants. The space defined by these determinants was partitioned into singlet, triplet, and quintuplet subspaces. From the singlet space we projected the $^1A_1$ and $^1B_1$ functions, while from the triplet space we projected only the $^3B_1$. We did not consider the quintuplet subspaces, and because of digital computer limitations we deleted from consideration primary structures 1 and 20. Physically, this is not a significant restriction. The 18 structures employed are listed in Table V. VB structures constructed from this set are shown in Table VI. The linear variation problem for the states $^3B_1$, $^1A_1$, and $^1B_1$ was solved for several values of the H–C–H angle, and the results are presented in Figure 3 as curves $^3B_1$(II), $^1A_1$(II), and $^1B_1$(II). The energies used in constructing these curves are presented in Table VII. (Wave functions are not tabulated but are available upon request.) We note that this rather extensive calculation predicts the $^3B_1$ lowest at all angles while calculation VB I predicted that the multiplicity of the ground state would change from triplet to singlet as the molecule is bent from the linear configuration.

(c) VB III. In the third calculation we use exactly the same VB structures as in calculation II. However, we modify the atomic basis slightly by scaling the hydrogen atom exponents by 1.8 (effective exponential H scaling of $\sqrt{1.8}$). This scaling factor, or values close to it, has been found optimum for hydrocarbons in this and several other laboratories. The results are

(5) J. L. Whitten and L. C. Allen, *J. Chem. Phys.*, **43**, S170 (1965); J. L. Whitten, *ibid.*, **44**, 359 (1966).

Table II. Valence-Bond Structures in Primary Structure Notation VB—Doubly Occupied 1s and 2s

	Valence-Bond Structures for $^1A_2$ State
1)	(1,4) + (4,1)
2)	(2,4) + (4,2)
3)	(5,7) + (7,5)
4)	(5,9) + (9,5)
5)	(6,10) + (10,6)
6)	(8,10) + (10,8)
7)	2.0 (1,10) + 2.0 (10,1) − (4,6) − (6,4) + (3,7) + (7,3)
8)	2.0 (3,7) + 2.0 (7,3) + (1,10) + (10,1) + (4.6) + (6,4)
9)	2.0 (3,9) + 2.0 (9,3) + (2,10) + (10,2) + (4,8) + (8,4)
10)	2.0 (2,10) + 2.0 (10,2) − (4,8) − (8,4) + (3,9) + (9,3)

	Valence-Bond Structures for $^3A_1$ State
1)	(1,2) − (2,1)
2)	(1,6) − (6,1)
3)	(2,8) − (8,2)
4)	(4,10) − (10,4)
5)	(6,8) − (8,6)
6)	(7,9) − (9,7)
7)	(1,8) − (8,1)
8)	(2,6) − (6,2)
9)	(3,5) − (5,3)

	Valence-Bond Structures for $^1A_1$ State
1)	(1,1)
2)	(2,2)
3)	(3,3)
4)	(4,4)
5)	(5,5)
6)	(6,6)
7)	(7,7)
8)	(8,8)
9)	(9,9)
10)	(10,10)
11)	(1,2) + (2,1)
12)	(1,6) + (6,1)
13)	(2,8) + (8,2)
14)	(4,10) + (10,4)
15)	(6,8) + (8,6)
16)	(7,9) + (9,7)
17)	2.0 (1,8) + 2.0 (8,1) + (2.6) + (6,2) − (3,5) − (5,3)
18)	2.0 (2,6) + 2.0 (6,2) + (3,5) + (5,3) + (1,8) + (8,1)

	Valence-Bond Structures for $^1B_2$ State
1)	(1,3) + (3,1)
2)	(1,5) + (5,1)
3)	(2,3) + (3,2)
4)	(2,5) + (5,2)
5)	(3,6) + (6,3)
6)	(3,8) + (8,3)
7)	(4,7) + (7,4)
8)	(4,9) + (9,4)
9)	(5,6) + (6,5)
10)	(5,8) + (8.5)
11)	(7,10) + (10,7)
12)	(9,10) + (10,9)

	Valence-Bond Structures for $^1B_1$ State
1)	(1,7) + (7,1)
2)	(2,9) + (9,2)
3)	(3,4) + (4,3)
4)	(3,10) + (10,3)
5)	(6,7) + (7,6)
6)	(8,9 + (9,8)
7)	2.0 (1,9) + 2.0 (9,1) − (4,5) − (5,4) + (2,7) + (7,2)
8)	2.0 (2,7) + 2.0 (7,2) + (1,9) + (9,1) + (4,5) + (5,4)
9)	2.0 (5,10) + 2.0 (10,5) − (7,8) − (8,7) + (6,9) + (9,6)
10)	2.0 (6,9) + 2.0 (9,6) + (5,10) + (10,5) + (7,9) + (8,7)

	Valence-Bond Structures for $^3B_2$ State
1)	(1,3) − (3,1)
2)	(1,5) − (5,1)
3)	(2,3) − (3,2)
4)	(2,5) − (5,2)
5)	(3,6) − (6,3)
6)	(3,8) − (8,3)
7)	(4,7) − (7,4)
8)	(4,9) − (9,4)
9)	(5,6) − (6,5)
10)	(5,8) − (8,5)
11)	(7,10) − (10,7)
12)	(9,10) − (10,9)

	Valence-Bond Structures for $^3A_2$
1)	(1,4) − (4,1)
2)	(2,4) − (4,2)
3)	(5,7) − (7,5)
4)	(5,9)′ − (9,5)
5)	(6,10) − (10,6)
6)	(8,10) − (10,8)
7)	(1,10) − (10,1)
8)	(4,6) − (6,4)
9)	(3,7) − (7,3)
10)	(2,10) − (10,2)
11)	(4,8) − (8,4)
12)	(3,9) − (9,3)

	Valence-Bond Structures for $^3B_1$ State
1)	(1,7) − (7,1)
2)	(2,9) − (9,2)
3)	(3,4) − (4,3)
4)	(3,10) − (10,3)
5)	(6,7) − (7,6)
6)	(8,9) − (9,8)
7)	(1,9) − (9,1)
8)	(4,5) − (5,4)
9)	(2,7) − (7,2)
10)	(5,10) − (10,5)
11)	(7,8) − (8,7)
12)	(6,9) − (9,6)

Table III. Energy[a] *vs.* Angle for Methylene VB—Doubly Occupied 1s and 2s (R_{CH} = 2.00 Bohrs)

θ, deg	$^1A_1$	$^1A_2$	$^1B_1$	$^1B_2$	$^3A_1$	$^3A_2$	$^3B_1$	$^3B_2$
80	−38.7474	−38.5693	−38.5819	−38.2780	−38.2483	−38.6021	−38.6266	−38.3926
100	−38.7559	−38.5347	−38.6382	−38.3052	−38.2642	−38.5671	−38.6860	−38.4096
120	−38.7355	−38.4789	−38.6618	−38.3109	−38.3283	−38.5118	−38.7122	−38.4015
140	−38.6977	−38.4105	−38.6642	−38.3052	−38.3943	−38.4441	−38.7177	−38.3783
160	−38.6593	−38.3379	−38.6547	−38.2960	−38.4397	−38.3724	−38.7119	−38.5471
180	−38.6437	−38.2915	−38.6477	−38.2915	−38.4555	−38.3275	−38.7072	...

[a] Energy in Hartree units.

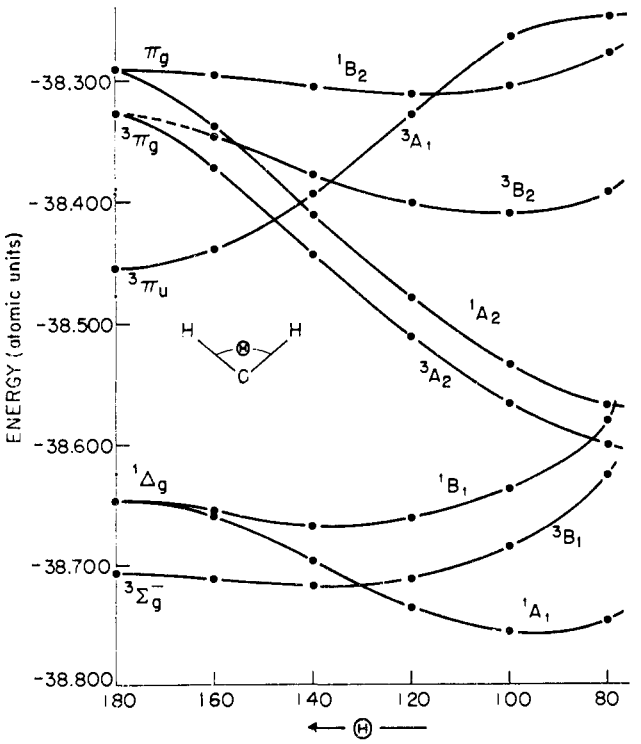

Figure 2. Energy *vs.* angle for various states of CH_2. VB—doubly occupied 1s and 2s.

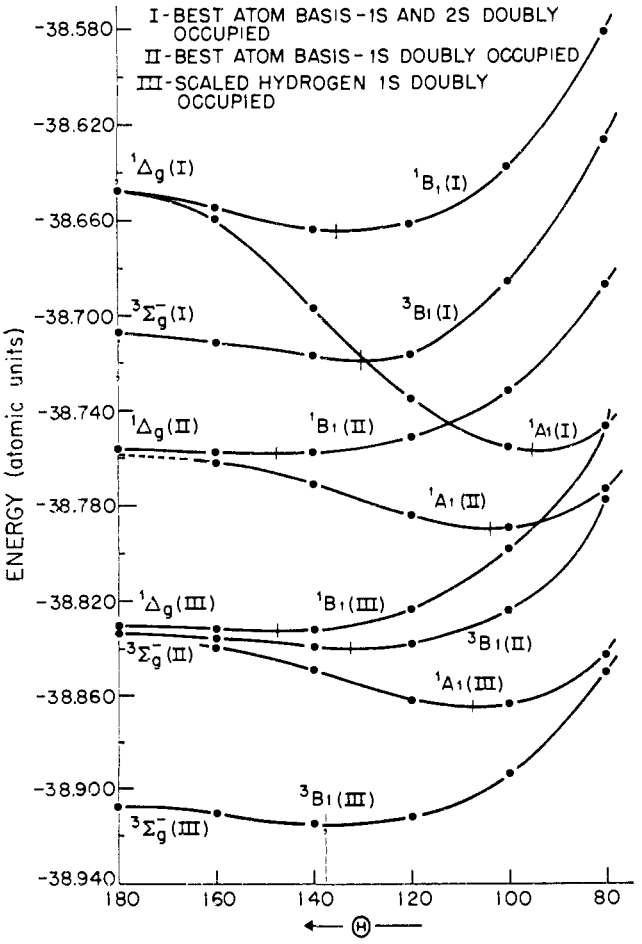

Figure 3. Energy *vs.* angle for the $^3B_1$, $^1B_2$, and $^1A_1$ states of CH_2. A comparison of three levels of VB calculations.

Table IV. Energy Spectrum of Linear Methylene VB—Doubly Occupied 1s and 2s

Linear	Bent[a]	Energy[b]	ΔE, eV
$^3\Sigma_g^-$	$^3B_1$	−38.7072	0.0000
$^1\Delta_g$	$^1A_1$, $^1B_1$	−38.6473	1.6299
$^1\Sigma_g^+$	$^1A_1$	−38.5909	4.1645
$^3\pi_u$	$^3A_1$, $^3B_1$	−38.4555	6.8488
$^1\pi_u$	$^1A_1$, $^1B_1$	−38.4235	7.7195
$^3\pi_g$	$^3A_2$, $^3B_2$	−38.3275	10.3316
$^1\pi_g$	$^1A_2$, $^1B_2$	−38.2915	11.3112
$^3\Sigma_u^-$	$^3A_2$	−38.2375	12.7805
$^3\Delta_u$	$^3A_2$, $^3B_2$	−38.2156	13.3764
$^1\Sigma_u^-$	$^1A_2$	−38.2005	13.7873
$^3\Sigma_u^+$	$^3B_2$	−38.1592	14.9111
$^1\Delta_u$	$^1B_2$, $^1A_2$	−38.0063	19.0715
$^1\Sigma_u^+$	$^1B_2$	−37.9489	20.6333
$^3\Delta_g$	$^3A_1$, $^3B_1$	−37.7168	26.9488
$^1\Sigma_g^-$	$^1B_1$	−37.7017	27.3597
$^3\Sigma_g^+$	$^3A_1$	−37.6598	28.4998

[a] Bent molecules states correlated with linear symmetries. [b] Energy in Hartree units.

Table V. Atomic Basis and Primary Structures Used in Both VB—Doubly Occupied 1s Only and VB—Doubly Occupied 1s with Scaled Hydrogen

Atomic Basis
1) Carbon 1s
2) Carbon 2s
3) Hydrogen 1 1s + hydrogen 2 1s
4) Carbon p_x
5) Carbon p_z
6) Hydrogen 1 1s − hydrogen 2 1s
7) Carbon p_y

Complete Set of Primary Structures for Basis Orbitals Used					Primary Structures Actually Employed in Calculation[a]				
1)	1	2	3	4	1)	1	2	5	6
2)	1	2	3	5	2)	1	3	5	6
3)	1	2	3	6	3)	1	5	6	4
4)	1	2	3	7	4)	1	2	3	7
5)	1	2	4	5	5)	1	2	4	7
6)	1	2	4	6	6)	1	3	4	7
7)	1	2	4	7	7)	1	2	5	7
8)	1	2	5	6	8)	1	2	6	7
9)	1	2	5	7	9)	1	3	5	7
10)	1	2	6	7	10)	1	3	6	7
11)	1	3	4	5	11)	1	5	4	7
12)	1	3	4	6	12)	1	6	4	7
13)	1	3	4	7	13)	1	2	3	5
14)	1	3	5	6	14)	1	2	3	6
15)	1	3	5	7	15)	1	2	5	4
16)	1	3	6	7	16)	1	2	6	4
17)	1	4	5	6	17)	1	3	5	4
18)	1	4	5	7	18)	1	3	6	4
19)	1	4	6	7					
20)	1	5	6	7					

[a] Structures have been renumbered.

shown in Figure 3 as curves $^3B_1$(III), $^1A_1$(III), and $^1B_1$(III). The energy values and wave functions used to construct these curves are given in Tables VII and VIII, respectively. We see that in relation to calculation II the energy has improved, but the qualitative features are unchanged.

D. Molecular Orbital Considerations. We obtained the single determinant solution to the Hartree–Fock–Roothaan equations for the $^1A_1$ state. The solution was obtained as a function of angle using the carbon group orbital basis[5] with scaled hydrogen exponents. The scaling factor ($\eta^2 = 1.8$) is the same as was used in VB III. The one-electron energies are plotted as a function of angle in Figure 4. We note the general

Table VI. Valence-Bond Structures in Primary Structure Notation Used in Both VB—Doubly Occupied 1s Only and VB—Doubly Occupied 1s with Scaled Hydrogen

	Triplet B_1 State		
1)	(13,7) − (7,13)	22)	(17,12) − (12,17)
2)	(13,9) − (9,13)	23)	(18,11) − (11,18)
3)	(14,8) − (8,14)	24)	(6,3) − (3,6)
4)	(14,10) − (10,14)	25)	(15,9) − (9,15)
5)	(15,7) − (7,15)	26)	(7,17) − (17,7)
6)	(15,11) − (11,15)	27)	(14,12) − (12,14)
7)	(16,8) − (8,16)	28)	(16,10) − (10,16)
8)	(16,12) − (12,16)	29)	(8,18) − (18,8)
9)	(17,9) − (9,17)	30)	(1,5) − (5,1)
10)	(17,11) − (11,17)	31)	(15,8) − (8,15)
11)	(18,10) − (10,18)	32)	(7,16) − (16,7)
12)	(18,12) − (12,18)	33)	(2,6) − (6,2)
13)	(13,11) − (11,13)	34)	(17,10) − (10,17)
14)	(14,7) − (7,14)	35)	(9,18) − (18,9)
15)	(4,1) − (1,4)	36)	(13,12) − (12,13) + (14,11) − (11,14)
16)	(13,10) − (10,13)	37)	(4,3) − (3,4) + (1,6) − (6,1)
17)	(14,9) − (9,14)	38)	(1,6) − (6,1) + (15,10) − (10,15)
18)	(4,2) − (2,4)	39)	(15,10) − (10,15) + (7,18) − (18,7)
19)	(15,12) − (12,15)	40)	(16,9) − (9,16) + (8,17) − (17,8)
20)	(16,11) − (11,16)	41)	(8,17) − (17,8) + (5,2) − (2,5)
21)	(5,3) − (3,5)	42)	(7,18) − (18,7) + (16,9) − (9,16)
	Singlet B_1 State		
1)	(13,7) + (7,13)	15)	(13,10) + (10,13) + (14,9) + (9,14)
2)	(13,9) + (9,13)	16)	(4,2) + (2,4) + (14,9) + (9,14)
3)	(14,8) + (8,14)	17)	(15,12) + (12,15) + (16,11) + (11,16)
4)	(14,10) + (10,14)	18)	(5,3) + (3,5) + (16,11) + (11,16)
5)	(15,7) + (7,15)	19)	(17,12) + (12,17) + (18,11) + (11,18)
6)	(15,11) + (11,15)	20)	(6,3) + (3,6) + (18,11) + (11,18)
7)	(16,8) + (8,16)	21)	(13,11) + (11,13) + (15,9) + (9,15)
8)	(16,12) + (12,16)	22)	(7,17) + (17,7) + (15,9) + (9,15)
9)	(17,9) + (9,17)	23)	(14,12) + (12,14) + (16,10) + (10,16)
10)	(17,11) + (11,17)	24)	(8,18) + (18,8) + (16,10) + (10,16)
11)	(18,10) + (10,18)	25)	(1,5) + (5,1) + (15,8) + (8,15)
12)	(18,12) + (12,18)	26)	(7,16) + (16,7) + (15,8) + (8,15)
13)	(13,8) + (8,13) + (14,7) + (7,14)	27)	(2,6) + (6,2) + (17,10) + (10,17)
14)	(4,1) + (1,4) + (14,7) + (7,14)	28)	(9,18) + (18,9) + (17,10) + (10,17)
	Singlet A_1 State		
1)	(13,13)	25)	(4,6) + (6,4)
2)	(14,14)	26)	(1,2) + (2,1)
3)	(4,4)	27)	(1,3) + (3,1)
4)	(1,1)	28)	(15,16) + (16,15)
5)	(15,15)	29)	(15,17) + (17,15)
6)	(7,7)	30)	(7,8) + (8,7)
7)	(16,16)	31)	(7,9) + (9,7)
8)	(8,8)	32)	(7,11) + (11,7)
9)	(5,5)	33)	(16,18) + (18,16)
10)	(2,2)	34)	(8,10) + (10,8)
11)	(17,17)	35)	(8,12) + (12,8)
12)	(9,9)	36)	(5,6) + (6,5)
13)	(18,18)	37)	(2,3) + (3,2)
14)	(10,10)	38)	(17,18) + (18,17)
15)	(6,6)	39)	(9,10) + (10,9)
16)	(3,3)	40)	(9,11) + (11,9)
17)	(11,11)	41)	(10,12) + (12,10)
18)	(12,12)	42)	(11,12) + (12,11)
19)	(13,14) + (14,13)	43)	(13,16) + (16,13) + (14,15) + (15,14)
20)	(13,15) + (15,13)	44)	(13,18) + (18,13) + (14,17) + (17,14)
21)	(13,17) + (17,13)	45)	(15,18) + (18,15) + (16,17) + (17,16)
22)	(14,16) + (16,14)	46)	(7,10) + (10,7) + (8,9) + (9,8)
23)	(14,18) + (18,14)	47)	(7,12) + (12,7) + (8,11) + (11,8)
24)	(4,5) + (5,4)	48)	(9,12) + (12,9) + (10,11) + (11,10)

agreement of $3a_1$ and $2b_2$ curves with those presented by Walsh.[6] The $2a_1$ MO has the form

$$|2a_1\rangle = \alpha|h1 + h2\rangle + \beta(|2s\rangle + \lambda|p_z\rangle)$$

with $\alpha, \beta, \lambda > 0$. This orbital is very much involved in the binding. (The $1a_1$ molecular orbital is essentially the carbon 1s and is chemically uninteresting.) In the linear configuration, $\lambda = 0$. As the molecule is bent the carbon sp hybrid interacts with the symmetric combination of hydrogen orbitals causing electron density to be built up in the region between the carbon and hydrogen atoms. As the molecule is bent from 180 to 90°, this orbital becomes more stable. The $1b_2$ orbital has the form (with δ and $\epsilon > 0$)

$$|1b_2\rangle = \delta|h2 - h1\rangle - \epsilon|p_z\rangle$$

(6) A. D. Walsh, *J. Chem. Soc.*, 2260 (1953).

Table VII. Energy[a] *vs.* Angle for Methylene VB—Doubly Occupied 1s Only

θ, deg	$^3B_1$ Free atom hydrogen	$^3B_1$ Scaled hydrogen	$^1A_1$ Free atom hydrogen	$^1A_1$ Scaled hydrogen	$^1B_1$ Free atom hydrogen	$^1B_1$ Scaled hydrogen
80	−38.7871	−38.8505	−38.7736	−38.8429	−38.6875	−38.7471
100	−38.8243	−38.8939	−38.7898	−38.8643	−38.7321	−38.7988
120	−38.8382	−38.9123	−38.7843	−38.8622	−38.7518	−38.8239
140	−38.8395	−38.9151	−38.7712	−38.8491	−38.7580	−38.8322
160	−38.9354	−38.9105	−38.7625	−38.8395	−38.7576	−38.8318
180	−38.8329	−38.9075	...	...	−38.7565	−38.8304

[a] Energy in Hartree units.

This orbital has a node along the C_2 axis and becomes less stable as the molecule is bent from 180 to 90°. Since a charge density contour cannot pass across the nodal plane containing the C_2 axis, the electrons in this orbital are essentially localized in the regions of the CH bonds, and the destabilization of the orbital upon bending may be interpreted as bond–bond repulsion.

The $3a_1$ orbital is the highest occupied MO for the $^1A_1$ state. This orbital has the form

$$|3a_1\rangle = -\eta|h2 + h1\rangle + \kappa(|1s\rangle - \mu|p_z\rangle)$$

with $\eta, \kappa, \mu > 0$. In the linear configuration this MO is a pure carbon p_π orbital and is nonbonding. As the molecule is bent from the linear configuration, the hydrogen atoms experience a net attraction due to the symmetric combination of the 1s orbitals. As the molecule is bent the orbital becomes more stabilized. The $3a_1$ orbital may be thought of as describing a hydrogen molecule interacting with a sp-hybridized carbon atom, the sp hybridization being such that the maximum of the electron density is along the $-x$ axis. The first virtual orbital is the $1b_1$ which is the $p_{\pi y}$ orbital of carbon.

The single determinant $^1A_1$ state is defined by the configuration $(1a_1)^2(2a_1)^2(1b_2)^2(3a_1)^2$. Single excitation into the $1b_1$ level yields the configuration $(1a_1)^2(2a_1)^2(1b_2)^2(3a_1)^1(1b_1)^1$, from which we may construct the $^3B_1$ and $^1B_1$ states. It is expedient to write these MO functions in the primary structure notation. We therefore define

Primary structure	Orbital characterization
1	$1a_1\ 2a_1\ 3a_1\ 1b_2$
2	$1a_1\ 2a_1\ 1b_2\ 1b_1$

In this notation we have

$$|^1A_1\rangle = (1,1) \quad (1)$$

$$|^1B_1\rangle = (1,2) + (2,1) \quad (2)$$

$$|^3B_1\rangle = (1,2) - (2,1) \quad (3)$$

The energy as calculated with these functions is presented in Table IX and plotted in Figure 5 along with the results of calculation VB III for comparison. Particularly interesting is the similarity in the curvature of the variationally determined VB III energy curves obtained by using virtual orbitals. Since the carbon b_1 MO is the p_π orbital, its atomic character is maintained inviolate for all angles. Excitation into this first virtual orbital is therefore rather unique, and one would not expect the parallelism between the VB determined curve

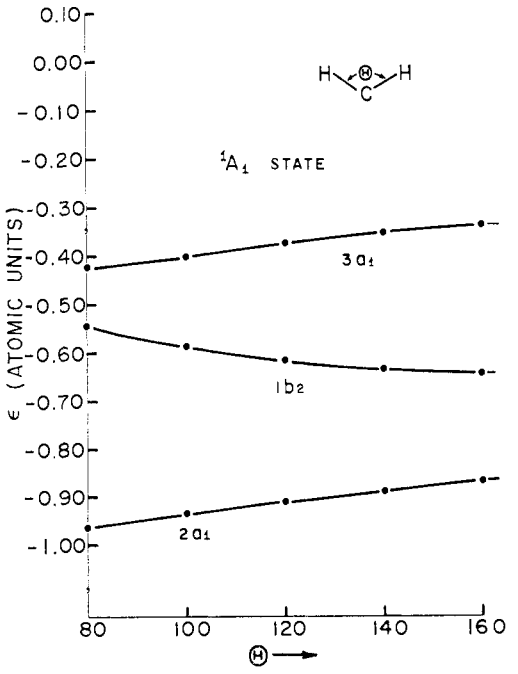

Figure 4. One-electron energies of the $^1A_1$ state of CH_2 *vs.* angle (Walsh diagram).

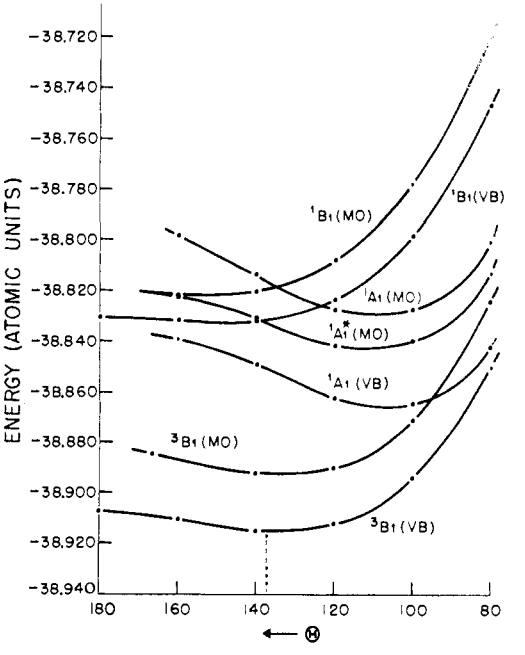

Figure 5. Energy *vs.* angle for the $^3B_1$, $^1B_1$, and $^1A_1$ states of CH_2. The VB calculation has the 1s doubly occupied and scaled hydrogens ($\eta = \sqrt{1.8}$).

Table VIII. Valence-Bond Wave Functions for Methylene (Doubly Occupied 1s and Scaled Hydrogen)

VB struct	$\theta = 100°$	$\theta = 120°$	$\theta = 140°$	$\theta = 160°$	VB struct	$\theta = 100°$	$\theta = 120°$	$\theta = 140°$	$\theta = 160°$
				$^3B_1$ State					
1	0.098631	0.080754	0.062220	0.035925	22	−0.020914	−0.018669	−0.014765	−0.008474
2	0.014225	0.009094	0.006979	0.004352	23	−0.036816	−0.031609	−0.024313	−0.013761
3	0.047998	0.044390	0.035890	0.020955	24	0.000597	0.000334	0.000160	0.000061
4	−0.027802	−0.022158	−0.016633	−0.009528	25	−0.127348	−0.120756	−0.120793	−0.123568
5	−0.035915	−0.043865	−0.051084	−0.057285	26	0.077361	0.088256	0.103503	0.118484
6	0.022971	0.021100	0.016655	0.009472	27	−0.018054	−0.015297	−0.012094	−0.009479
7	−0.077863	−0.084385	−0.089860	−0.095576	28	−0.029877	−0.024638	−0.017878	−0.012012
8	0.012538	0.008412	0.005255	0.002689	29	0.019607	0.017920	0.014521	0.011087
9	−0.027095	−0.033564	−0.043466	−0.053486	30	0.002145	0.001500	0.000997	0.000702
10	0.033100	0.030519	0.025430	0.015270	31	0.166649	0.165705	0.164154	0.163788
11	0.008144	0.009080	0.010871	0.012900	32	−0.141748	−0.148902	−0.155198	−0.161192
12	0.004278	0.002750	0.001283	0.000368	33	0.001615	0.001167	0.000826	0.000626
13	−0.062866	−0.051708	−0.044691	−0.040320	54	0.004044	0.005747	0.006997	0.007560
14	−0.092884	−0.081066	−0.063635	−0.036559	35	0.002698	0.000640	−0.003994	−0.006624
15	0.001255	0.000929	0.000606	0.000304	36	0.067891	0.068136	0.070219	0.073018
16	−0.048088	−0.041393	−0.032815	−0.019192	37	−0.008460	−0.008013	−0.007785	−0.007772
17	−0.021983	−0.020977	−0.017832	−0.010849	38	0.020083	0.020233	0.020605	0.021181
18	−0.001935	−0.001385	−0.000880	−0.000432	39	0.125665	0.125956	0.128711	0.132456
19	−0.061277	−0.048352	−0.034094	−0.018084	40	−0.122593	−0.128754	−0.137599	−0.146768
20	−0.045958	−0.034409	−0.022857	−0.011544	41	0.022399	0.020159	0.018545	0.017818
21	−0.001764	−0.001196	−0.000719	−0.000339	42	0.328561	0.346797	0.371916	0.397381
				$^1A_1$ State					
1	−0.032938	−0.018136	−0.006679	−0.000303	25	0.006040	0.006339	0.006331	0.004592
2	0.004105	0.001170	0.000075	0.000044	26	0.012378	0.010487	0.006601	0.001973
3	−0.008481	−0.014054	−0.024885	−0.042062	27	−0.006693	−0.005017	−0.003468	−0.001608
4	0.025418	0.016641	0.007805	0.000943	28	0.222356	0.243448	0.253586	0.228921
5	−0.052313	−0.056330	−0.057047	−0.049730	29	−0.105902	−0.127126	−0.148555	−0.147597
6	0.010635	0.015420	0.025653	0.042839	30	−0.046260	−0.068585	−0.114874	−0.191384
7	−0.093542	−0.094116	−0.090522	−0.077663	41	0.038801	0.050959	0.079775	0.128475
8	0.019022	0.029504	0.049641	0.081184	32	−0.003613	−0.005115	−0.006421	−0.005682
9	0.002978	0.003122	0.002686	0.001123	33	−0.031410	−0.028516	−0.021767	−0.013822
10	−0.000136	0.000366	0.000340	0.000063	34	0.005311	0.006374	0.007364	0.007767
11	−0.015528	−0.026924	−0.040077	−0.046193	35	−0.005381	−0.004641	−0.003797	−0.002264
12	0.015939	0.017618	0.025724	0.041917	36	0.004761	0.004275	0.002952	−0.000477
13	0.004835	0.006303	0.008125	0.008782	37	0.011229	0.008642	0.005533	0.002288
14	−0.003027	−0.003063	−0.004526	−0.007546	38	−0.002231	0.002293	0.007208	0.009637
15	−0.006111	−0.005631	−0.002891	−0.002816	39	−0.004769	−0.006029	−0.007485	−0.010095
16	0.010840	0.012429	0.013035	0.011786	40	−0.034636	−0.030237	−0.026102	−0.016819
17	0.011038	0.010878	0.008660	0.002317	41	−0.004584	−0.003628	−0.001829	−0.000094
18	0.010405	0.008589	0.005171	−0.000195	42	−0.032495	−0.031145	−0.023991	−0.006356
19	0.016602	0.012028	0.005602	0.002189	43	−0.251810	−0.206945	−0.148327	−0.069403
20	0.123536	0.091872	0.062458	0.028669	44	−0.011190	−0.010909	−0.009502	−0.004876
21	0.027216	0.023345	0.018867	0.009664	55	0.201407	0.236463	0.265543	0.255844
22	0.041641	0.036584	0.026088	0.011792	46	−0.065287	−0.089105	−0.139339	−0.221027
23	−0.007367	−0.006235	−0.004865	−0.002455	47	0.014557	0.016602	0.018469	0.015100
24	0.006266	0.005279	0.003850	0.001802	48	0.055699	0.049808	0.040515	0.023079
				$^1B_1$ State					
1	0.095722	0.074151	0.054363	0.030154	15	−0.046540	−0.039904	−0.030440	−0.016828
2	0.003792	0.002553	0.003355	0.002948	16	0.005273	0.003363	0.001963	0.000901
3	0.038151	0.034490	0.026331	0.014406	17	−0.135074	−0.109390	−0.078279	−0.041508
4	−0.028329	−0.022404	−0.015906	−0.008414	18	0.008313	0.006567	0.004532	0.002323
5	0.011784	0.016669	0.022543	0.027792	19	−0.003191	−0.002821	−0.002909	−0.002161
6	−0.015705	−0.013683	−0.010383	−0.005654	20	−0.005342	−0.004043	−0.002712	−0.001375
7	−0.030122	−0.022550	−0.013554	−0.006787	21	−0.054168	−0.033179	−0.016695	−0.004692
8	−0.024578	−0.023716	−0.018836	−0.010442	22	−0.265526	−0.299730	−0.340419	−0.377673
9	0.036648	0.038422	0.036712	0.033752	23	−0.015128	−0.009985	−0.005108	−0.001418
10	0.070032	0.062101	0.049118	0.028183	24	−0.159033	−0.171894	−0.182241	−0.190616
11	0.073192	0.081220	0.090288	0.098546	25	0.003112	0.002319	0.001279	0.000368
12	0.031963	0.026681	0.019301	0.010254	24	0.400567	0.430061	0.460179	0.487836
13	−0.129937	−0.113809	−0.091477	−0.053890	27	0.002192	0.001660	0.000953	0.000287
14	−0.024013	−0.019244	−0.013632	−0.007181	28	0.136716	0.152913	0.171098	0.186850

and that obtained by virtual excitations to be general.

The single determinant solution for the $^1A_1$ state becomes a very poor representation of this state as this molecule approaches a linear configuration. This is anticipated by noting that the $^1A_1$ state must correlate with the $^1\Delta_g$ state in the linear configuration, and a single determinant cannot represent the $^1\Delta_g$ state. In the linear configuration the functions (1,1) and (2,2) are degenerate since the $3a_1 \rightarrow \pi_x$ and $1b_1 \rightarrow \pi_y$ as $\theta \rightarrow 180°$. Therefore, the $^1A_1$ state is better represented as a mixture of (1,1) and (2,2) at all angles. We therefore formed

$$|^1A_1^*\rangle = \sin\lambda\,(1,1) + \cos\lambda\,(2,2) \qquad (4)$$

and varied λ at each angle θ. The energy as calculated with this function is shown in Table IX and plotted *vs.*

Table IX. Total Energy[a] *vs.* Angle for Methylene Molecular Orbital Calculation

θ, deg	$^1A_1$[b]	$^1A_1$*[c]	$^1B_1$[d]	$^3B_1$[d]
80	−38.8007	−38.8131	−38.7199	−38.8242
100	−38.8274	−38.8401	−38.7782	−38.8711
120	−38.8275	−38.8418	−38.8083	−38.8907
140	−38.8137	−38.8316	−38.8204	−38.8922
160	−38.7986	−38.8232	−38.8224	−38.8849

[a] Energy in Hartree units. [b] Single determinant SCF solution $(1a_1)^2(2a_1)^2(1b_2)^2(3a_1)^2$. [c] Variation calculation over two determinant bases, consisting of $(1a_1)^2(2a_1)^2(1b_2)^2(3a_1)^2$ and $(1a_1)^2(2a_1)^2(1b_2)^2(1b_1)^2$. [d] States are formed by a single excitation from the $3a_1$ MO to the $1b_1$ virtual orbital.

angle in Figure 5. It indeed behaves properly, becoming degenerate with the $^1B_1$, as the linear configuration is approached.

III. Discussion of Energy Results

A. Order of States and Geometry. We present in Table X the equilibrium angles and energies of the $^3B_1$, $^1A_1$, and $^1B_1$ states as predicted from the calculations we have described and for comparison the results of Foster and Boys.[7] We note the following.

(a) Every calculation (with the exception of VB I) predicts the order of the states as $^3B_1 < {}^1A_1 < {}^1B_1$ (VB I predicts $^1A_1 < {}^3B_1 < {}^1B_1$).

(b) Every calculation (with the exception of VB I) predicts the $^3B_1$ to be the ground state for all angles considered (VB I predicts that in going from the linear to the bent configuration the ground state will change from $^3B_1$ to $^1A_1$ at $\theta = 130°$).

(c) Every calculation predicts that the energy of the $^3B_1$ and $^1B_1$ states is a very weak function of θ for $\theta > 120°$. Indeed, in our best calculation (VB III) the energy separation $^3B_1(180°) - {}^3B_1(138°)$ is 0.19 eV, and $^1B_1(180°) - {}^1B_1(148°)$ is only 0.08 eV.

(d) Every calculation (with the exception of VB I) predicts that the energy separation between the $^3B_1$ and $^1A_1$ states increases monotonically with increasing HCH angle. In VB III the difference is 1.77 eV at $\theta = 138°$.

From the preceding observations we conclude that our calculations predict (i) the order of the states is $^3B_1 < {}^1A_1 < {}^1B_1$ for values of the HCH angle between 90 and 180°.

(ii) Because of the very flat potential curves of the $^3B_1$ and $^1B_1$ states, the predicted equilibrium angles of 138 and 148°, respectively, could be changed significantly with minor changes in the atomic bases. The calculated equilibrium angle of 108° for the $^1A_1$ state is more reliable. Thus our results are in over-all agreement with Herzberg's spectroscopic conclusion:[8] $^3B_1$ (~180°) < $^1A_1$(103°) < $^1B_1$(140°). With regard to detailed differences it seems reasonable to conclude that the theoretical and experimental values are at about the same level of conclusiveness and thus these differences remain as present uncertainties.

(iii) In view of (ii) we must give 1.77–2.10 eV as the range for the probable energy of the $^3B_1$–$^1A_1$ separation.

B. Heat of Atomization. The heats of atomization, ΔH, for the first three states of CH_2 are defined by the reactions (the precision of our calculations does not require distinction between energy and enthalpy)

$$CH_2(^3B_1) \longrightarrow C(^3P) + 2H(^2S) + \Delta H(^3B_1) \quad (A)$$

$$CH_2(^1A_1) \longrightarrow C(^1D) + 2H(^2S) + \Delta H(^1A_1) \quad (B)$$

$$CH_2(^1B_1) \longrightarrow C(^1D) + 2H(^2S) + \Delta H(^1B_1) \quad (C)$$

Experimental estimates for $\Delta H(^3B_1)$ have been obtained by considering the process

$$CH_2(^3B_1) \longrightarrow CH(^2\pi) + H(^2S) + \chi$$

and from spectroscopy[9] we know

$$CH(^2\pi) \longrightarrow C(^3P) + H(^2S) - 3.47 \text{ eV}$$

Therefore

$$\Delta H(^3B_1) = \chi(\text{eV}) - 3.47 \text{ eV}$$

Cottrell[10a] estimates $\chi \cong -5.2$ eV while Trotman-Dickenson[10b] gives $\chi \cong -4.8$ eV. We therefore have the estimates $\Delta H(^3B_1) \cong -8.7$ or -8.3 eV, and we take these as being indicative of the probable magnitude of the desired quantity. We present in Table XI the heats of atomization which we have calculated and for comparison the results of Foster and Boys.[7] The energy of the ^3P state of carbon in our atomic basis is −37.6805 Hartree units.[5] We calculate the ^1D energy to be −1.58 eV for the ^3P–^1D multiplet separation which is to be compared with the experimental value[11] of −1.26 eV. The data presented by Foster and Boys[7] yields −2.01 eV for this splitting. On the whole our best VB wave functions agree fairly well with the Foster and Boys results, and if we take −8.47 eV as a reasonable compromise between the two experimental estimates, the calculations yield respectively 75 and 76% of the heat of reaction.

C. Spectroscopy. (1) Experimental. Herzberg[8] has obtained the absorption spectra of CH_2 in the vacuum ultraviolet, visible, and near-ultraviolet. He finds (a) a band at 8.76 eV, the structure of which is typical of a $\Sigma \leftrightarrow \Sigma$ transition (Herzberg assigns this as $^3\Sigma_\mu^- \leftarrow {}^3\Sigma_g^-$ and concludes that both states involved in the transition are linear or very nearly so); (b) a many-lined spectrum between 1.305 and 2.25 eV (In this region bands are found at 1.513, 1.695, and 1.898 eV. These "red bands" are assigned rather definitely to the transition $^1B_1 \leftarrow {}^1A_1$.); (c) a series of very weak bands, between 3.54 and 3.87 eV, which are favored by the conditions under which the red bands are produced (Herzberg tentatively assigns these to the transition $^1A_1 \leftarrow {}^1A_1$).

2. Theoretical Prediction of Triplet–Triplet Transitions. From Figure 3 we see that VB I predicts the lowest triplet to be $^3B_1$ with an equilibrium angle of 130° and that two states, $^3A_2$ and $^3A_1$, are accessible *via* electric dipole transition from this $^3B_1$ state. The vertical excitation energies are

(7) J. M. Foster and S. F. Boys, *Rev. Mod. Phys.*, **26**, 716 (1957).
(8) G. Herzberg, *Proc. Roy. Soc.* (London), **A262**, 291 (1961); **A295**, 107 (1966).
(9) G. Herzberg, "Spectra of Diatomic Molecules," 2nd ed, D. Van Nostrand Co., New York, N. Y., 1950.
(10) (a) T. L. Cottrell, "The Strengths of Chemical Bonds," 2nd ed, Butterworth & Co., Ltd., London, 1958; (b) A. F. Trotman-Dickenson, *Ann. Rept.*, **55**, 36 (1958).
(11) C. Moore, "Atomic Energy Levels," Vol. 1, National Bureau of Standards Circular No. 467, U. S. Government Printing Office, Washington, D. C.

Table X. Equilibrium Angles and Energies for Various Methylene Wave Functions

		VB[a]					
		Doubly occ 1s and 2s	Doubly occ 1s only	Doubly occ 1s, scaled H's	MO[b]	Expt[c]	Foster and Boys[d]
$^1B_1$	θ_{min}, deg	135	148	148	154	140 ± 15	132
	Energy[e]	−38.665	−38.758	−38.833	−38.822	...	−38.808
$^1A_1$	θ_{min}, deg	95	104	108	111	102.4	90
	Energy	−38.757	−38.790	−38.864	−38.843		−38.865
$^3B_1$	θ_{min}, deg	130	132	138	133	180	129
	Energy	−38.720	−38.840	−38.915	−38.893		−38.904

[a] C–H distance taken as 2.00 au. [b] The $^1A_1$ state used is constructed from a variation calalculation over the two determinants defined by the configurations $(1a_1)^2(2a_1)^2(1b_1)^2(3a_1)^2$ and $(1a_1)^2(2a_1)^2(1b_1)^2(1b_1)^2$; the $^1B_1$ and $^3B_1$ states are constructed from the configuration $(1a_1)^2(2a_1)^2(1b_1)^2(3a_1)^1(1b_2)^1$ formed by exciting an electron from the $3a_1$ MO to the $1b_2$ virtual orbital. [c] The experimental data are from G. Herzberg, ref 8. This reference lists the experimental CH distances as $^1A_1$ = 2.10, $^1B_1$ = 1.98, $^3B_1$ = 1.95 au. [d] CH distance for $^1B_1$ and $^3B_1$ is 2.11 au; for $^1A_1$ it is 2.21 au: J. M. Foster and S. F. Boys, *Rev. Mod. Phys.*, **32**, 305 (1960). [e] Energy in Hartree units.

Table XI. Heats of Reactions from Various Methylene Wave Functions

	VB					
Reaction	Doubly occ 1s and 2s	Doubly occ 1s only	Doubly occ 1s, scaled H MO*[2]		Foster and Boys[b]	Expt
A	−1.06	−4.33	−6.36	−5.77	−6.42	−8.67, −8.27
B	−3.67	−4.57	−6.58	−6.01	−7.37	?
C	−1.17	−3.70	−5.74	−5.44	−5.83	?

[a] The $^1A_1$ state constructed by a variational calculation over the two determinants defined by the configurations $(1a_1)^2(2a_1)^2(1b_2)^2(3a_1)^2$ and $(1a_1)^2(2a_1)^2(1b_2)^2(1b_1)^2$ was used. The $^1B_1$ and $^3B_1$ states where constructed from the configuration resulting from a single excitation out of the $3a_1$ MO to the $1b_1$ virtual orbital. [b] J. M. Foster and S. F. Boys, *Rev. Mod. Phys.*, **32**, 305 (1960).

$$^3A_2 \longleftarrow {}^3B_1 \quad 6.6 \text{ eV } (z \text{ polarization})$$

$$^3A_1 \longleftarrow {}^3B_1 \quad 9.8 \text{ eV } (y \text{ polarization})$$

where the polarization of the transition is indicated relative to the coordinate system defined in Figure 1 (we note that the experimental transition should be z polarized).

In the linear configuration the three lowest states of $^3A_2$ symmetry correlate with the $^3\pi_g$, $^3\Sigma_u^+$, and $^3\Delta_u$ states which in this calculation lie respectively 10.3, 12.8, and 13.4 eV above the $^3\Sigma_g^-$ state. The three lowest states of $^3A_1$ symmetry correlate with the $^3\pi_u$, $^3\Delta_g$, and $^3\Sigma_g^+$ states of linear methylene, which in this calculation lie respectively 6.85, 26.9, and 28.5 eV above the $^3\Sigma_g^-$ state. Since excitation of a carbon 2p electron to a 3s, 3p, or 3d orbital requires approximately 7.5, 8.5, and 9.6 eV, respectively, we see that the inclusion of 3s, 3p, and 3d orbitals in our atomic basis set is necessary for an adequate representation of the (predominately Rydberg) $^3A_2$ and $^3A_1$ states.

The probable Rydberg character of the excited triplets, rapid variation of the energy *vs.* angle curves for the excited triplets, and the flatness of the $^3B_1$ curve together result in a large uncertainty in the prediction of the triplet–triplet transition energy.

3. Theoretical Prediction of Singlet–Singlet Transitions. The longest wavelength singlet–singlet transition is in all probability $^1B_1 \leftarrow {}^1A_1$. Vertical transition energies as predicted by our calculations are presented in Table XII. Also presented is the equilibrium angle of the $^1A_1$ state from which the transition originated. The adequacy with which our valence state represents the two singlet states involved in the transition is illustrated by the rather good agreement of our best calculation (VB III) with the experimental results.

In view of the reasonable agreement with experiment, we calculated the oscillator strength for the VB III and MO* functions (MO* refers to the $^1A_1$* state defined by eq 4). We take as our definition[12]

Table XII. Vertical Transition Energies for $^1A_1 \rightarrow {}^1B_1$

Calculation	ΔE[a]	Θ_{equil}[b], deg
VB—doubly occ 1s and 2s	3.41	95
VB—doubly occ 1s only	1.44	104
VB—doubly occ 1s and scaled H	1.52	108
MO[c]	0.98	107
MO*[d]	1.11	111
Exp[e]	1.51	102.4
	1.70	
	1.90	

[a] Energy in electron volts. [b] Equilibrium angle of $^1A_1$ state. [c] The $^1A_1$ state is $(1a_1)^2(2a_1)^2(1b_2)^2(2a_1)^2$; the $^1B_1$ arises from the configuration $(1a_1)^2(2a_1)^2(1b_2)^2(3a_1)^1(1b_1)^1$. [d] The $^1A_1$ state results from a variation calculation over the configurations $(1a_1)^2(2a_1)^2(1b_1)^2(3a_1)^2$ and $(1a_1)^2(2a_1)^2(1b_2)^2(1b_1)^2$.

$$f(^1B_1 \leftarrow {}^1A_1) = \frac{4\pi m}{3e^2\hbar}\nu|\vec{\mu}|^2$$

where m and e are respectively the electronic mass and charge, ν is the frequency of the transition, and $\vec{\mu}$ is the transition moment. All units are in the mks system. If we measure $\vec{\mu}$ in units of ea_0 and energy in Hartree units we have

$$f(^1B_1 \leftarrow {}^1A_1) = {}^2/_3(\Delta E)\mu_y^2$$

where

$$\Delta E = E(^1B_1) - E(^1A_1)$$

and

$$\mu_y = \langle {}^1B_1|\sum_{i=1}^{N} y_i|{}^1A_1\rangle$$

(12) J. C. Slater, "Quantum Theory of Atomic Structure," Vol. I, McGraw-Hill Book Co., Inc., New York, N. Y., 1960, p 156.

We present the oscillator strength, as a function of angle, in Table XIII. No experimental data are available for comparison. We note that even though ΔE for the MO* is smaller than for the VB, the larger transition moment as calculated with the MO* function causes the molecular orbital oscillator strength to be slightly larger than that calculated with the VB function.

Table XIII. Methylene Oscillator Strengths

θ, deg	$\langle {}^1A_1\|\mu_y\|{}^1B_1\rangle$[a]		ΔE[b]		$f({}^1B_1 \leftarrow {}^1A_1)$	
	VB[d]	MO*[c]	VB[d]	MO*[c]	VB[d]	MO*[c]
80	0.4000	0.4964	0.0958	0.0931	0.0102	0.0153
100	0.3277	0.4067	0.0655	0.0619	0.0047	0.0068
120	0.2438	0.2989	0.0383	0.0335	0.0015	0.0020
140	0.1321	0.1620	0.0169	0.0112	0.0002	0.0002

[a] Units of ea_0. [b] Hartree units. [c] The $^1A_1$ state was constructed by a variational calculation over the two determinants defined by the configurations $(1a_1)^2(2a_1)^2(1b_2)^2(3a_1)^2$ and $(1a_1)^2(2a_1)^2(1b_2)^2(1b_1)^2$; the $^1B_1$ state was constructed from the configuration resulting from a single excitation out of the $3a_1$ MO to the $1b_1$ virtual orbital. [d] VB functions with doubly occupied 1s and scaled hydrogen.

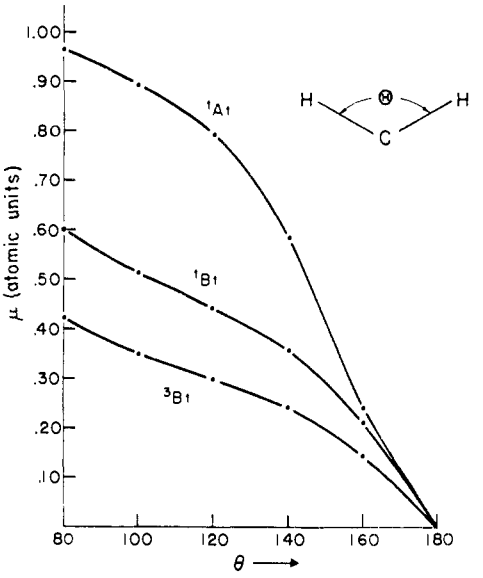

Figure 6. Dipole moment *vs.* angle for various states of CH_2. VB—doubly occupied 1s and scaled hydrogens.

IV. Properties

A. Dipole Moment. We take as our definition (in atomic units, ea_0)

$$\mu_\alpha = -\langle\psi|\sum_{i=1}^{8} r_{i\alpha}|\psi\rangle + \sum_{j=1}^{2} R_{j\alpha}$$

$$\alpha = x, y, z$$

with $r_{i\alpha}$ being the α coordinate of the ith electron and $R_{j\alpha}$ being the α coordinate of the jth nucleus. The coordinate system is as shown in Figure 1. By symmetry only μ_x is nonzero. We present in Table XIV the dipole moments of the $^1A_1$, $^1B_1$, and $^3B_1$ states as a function of the HCH angle for both the VB III and MO* functions. The graphical representation of these data is shown in Figures 6 and 7.

When one calculates the dipole moment curves for the $^1B_1$ and $^3B_1$ states using the MO* functions, one finds that the curves are identical. It is readily verified that when the $^1B_1$ and $^3B_1$ states are defined by eq 2 and 3 they yield identical expectation values for any one-electron operator. However, because the $^1B_1$ and $^3B_1$ states are predicted in the MO* representation to have different equilibrium angles, they are predicted

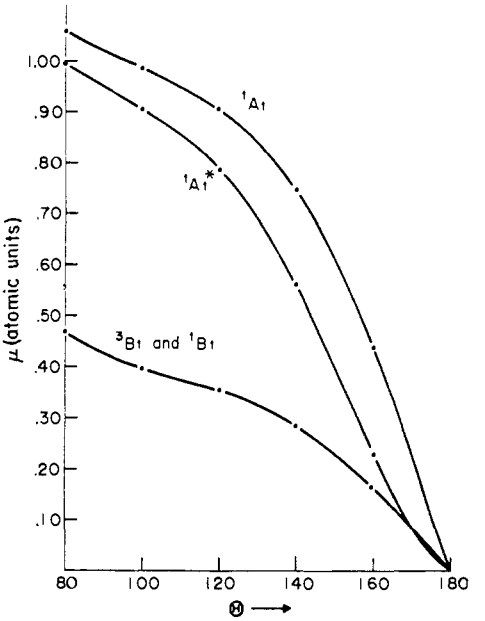

Figure 7. Dipole moment *vs.* angle for various states of CH_2. MO calculations.

Table XIV. Dipole Moments of Methylene[a]

θ, deg	MO		VB[d]			
	$^1A_1$* [b]	$^{1,3}B_1$[c]	$^1A_1$	$^1B_1$	$^3B_1$	$(^1B_1 + 3^3B_1)/4$
80	0.9951	0.4671	0.9654	0.6004	0.4227	0.4671
100	0.9041	0.3957	0.8922	0.5142	0.3502	0.3912
120	0.7866	0.3502	0.7919	0.4464	0.3003	0.3368
140	0.5617	0.2844	0.5829	0.3584	0.2420	0.2711
160	0.2289	0.1651	0.2411	0.2114	0.1441	0.1609
180	0.0000	0.0000	0.0000	0.0000	0.0000	0.0000

[a] μ_x (atomic units, ea_0, hydrogen side positive). [b] This state was constructed by a variational calculation over the two determinants defined by the configurations $(1a_1)^2(2a_1)^2(1b_2)^2(3a_1)^2$ and $(1a_1)^2(2a_1)^2(1b_2)^2(1b_1)^2$. [c] These states were constructed from the configurations formed by a single excitation out of the $3a_1$ MO to the $1b_1$ virtual orbital. [d] VB wave functions with doubly occupied 1s and scaled hydrogen.

to have different dipole moments. If we linearly interpolate the data presented in Table XIV to the predicted equilibrium angles of the various states, we obtain for the VB III calculation 0.852, 0.300, and 0.248 au for the dipole moments of the $^1A_1(108°)$, $^1B_1(148°)$, and $^3B_1(138°)$ states, respectively, and for the MO* calculation 0.840, 0.200, and 0.397 au for the $^1A_1(111°)$, $^1B_1(159°)$, and $^3B_1(133°)$, respectively. The VB and MO agree in their prediction for the $^1A_1$ state but give conflicting predictions for the order of the $^1B_1$ and $^3B_1$ states. Of course the predictions of the VB III calculation are preferred.

The fact that the dipole moment curve for the $^{1,3}B_1$ states as calculated in the MO* representation lies between the $^1B_1$ and $^3B_1$ curves as calculated with the VB III function lends itself to an interesting interpreta-

tion. If we suppose that the MO* result is a statistical mixture of the singlet and triplet dipole curves, then it should be representable as the average

$$\mu_{av}(B_1) = [\mu_x(^1B_1) + 3\mu_x(^3B_1)]/4$$

That this is indeed the situation, at least for small angles, is seen by the similarity of the last column in Table XIV to the MO*, $^{1,3}B_2$ results. The deviation at intermediate angles may be attributed to the decrease in the quality of the one-electron orbitals as the molecule approaches the linear configuration in which it would be an open-shell situation. The apparent agreement at $\theta = 160°$ might be attributed to the fact that both quantities must be equal to zero at 180°.

In order to understand why the dipole moment of the $^1A_1$ state is (at all angles) larger than the $^1B_1$ or $^3B_1$ dipoles, we will utilize the MO* representation. Accordingly we form the difference $\Delta\mu = \mu_x(^1A_1^*) - \mu_x(^{1,3}B_1)$

$$\Delta\mu = \langle {}^1A_1^* | -\sum_{i=1}^{8} x_i | {}^1A_1^* \rangle - \langle {}^{1,3}B_1 | -\sum_{i=1}^{8} x_i | {}^{1,3}B_1 \rangle$$

Using eq 2 or 3 with 4 we obtain

$$\Delta\mu = \cos 2\lambda \, \langle 3a_1 | x | 3a_1 \rangle$$

From the definition of λ in eq 4 we expect that as θ varies from 90 to 180°, λ varies from something greater than 90–135°. Therefore the cos 2λ is negative for values of θ less than 180° and zero at $\theta = 180°$. From the discussion in section II.D, we concluded that the average position of an electron in the $3a_1$ orbital was along the C_2 axis and on the $-x$ side. Therefore the integral $\langle 3a_1 | x | 3a_1 \rangle$ is negative and $\Delta\mu \geq 0$ for $90° < \theta < 180°$. A more physical argument is to note that the dipole moment is the difference between the sum of the x coordinates of the nuclei and the average position of an electron along the x axis. Because the average position of an electron in the $3a_1$ orbital is on the $-x$ axis, removing one of these electrons to form a B_1 configuration causes the average position to increase, thereby resulting in a smaller dipole moment for a B_1 state.

B. Second Moments of Charge Distribution and the Larmor Term in the Diamagnetic Susceptibility. We present in Table XV the expectation values of the operator

$$r_\alpha^2 = \frac{1}{8}\sum_{i=1}^{8} r_{i\alpha}^2$$

$$\alpha = x, y, \text{ and } z$$

for the $^1A_1$, $^1B_1$, and $^3B_1$ states as represented by the VB III wave function. The trends in these data may be understood by considering the change in the electron distribution which occurs when a $3a_1$ electron is promoted to a $1b_1$ orbital. By considering the form of the $3a_1$ orbital as discussed in section II.D, we see that this promotion ($a_1 \rightarrow b_1$) should result in a decrease in the electron density along the C_2 axis and thus a decrease in $\langle x^2 \rangle$, an increase in the electron density along the y axis and thus an increase in $\langle y^2 \rangle$, and a decrease in the electron density along the z axis and thus a decrease in $\langle z^2 \rangle$. We see that these expectations are quantitatively borne out by the data in Table XV. We also note the curious difference between the second moments of the $^1B_1$ and $^3B_1$ states. The $^1B_1$ seems to be more extended than the $^3B_1$ in the y direction but slightly less extended in the x and z directions.

The diamagnetic susceptibility, χ, is a sum of two contributions, χ^d, a diamagnetic (negative) term arising in first-order perturbation theory, and χ^p, a paramagnetic (positive) term arising in second-order perturbation theory.

$$\chi = \chi^d + \chi^p$$

We will consider only the diamagnetic contribution to χ. In general the diamagnetic term is a second-order tensor which in emu units is

$$\chi_{\alpha\beta}{}^d = (e^2/4mc^2)\langle \psi | \sum_{i=1}^{8} r_{i\alpha} r_{i\beta} - \delta_{\alpha\beta} r_i^2 | \psi \rangle$$

If we measure the integral in atomic units a_0^2 and use as our unit of susceptibility the erg/(G^2 mole), we have

$$\chi_{\alpha\beta}{}^d = (1.18845 \times 10^{-6})\langle \psi | \sum_{i=1}^{8} r_{i\alpha} r_{i\beta} - \delta_{\alpha\beta} r_i^2 | \psi \rangle \quad (5)$$

The Larmor term χ_L is defined as

$$\chi_L = {}^1/_3 \text{ trace } \chi_{\alpha\beta}$$

$$\chi_L = -0.7923 \times 10^{-6} \langle \psi | \sum_{i=1}^{8} r_i^2 | \psi \rangle$$

$$= -6.3384 \times 10^{-6} \langle r^2 \rangle$$

with $\langle r^2 \rangle = \langle x^2 \rangle + \langle y^2 \rangle + \langle z^2 \rangle$. If we consider the $^1A_1$ state at the calculated equilibrium angle, we have (with carbon as origin) $\langle r^2 \rangle = 3.1151$ au and therefore $\chi_L = -19.750 \times 10^{-6}$ erg/(G^2 mole), while the $^1B_1$ state yields $\langle r^2 \rangle = 3.0879$ au and from this $\chi_L = -19.57 \times 10^{-6}$ erg/(G^2 mole).

Unfortunately an experimental value for the diamagnetic susceptibility of free methylene is not known. Because of its fundamental importance in the interpretation of susceptibility data of organic compounds there have been many attempts at abstracting a sus-

Table XV. Second Moments of Charge Distribution[a] VB—Doubly Occupied 1s with Scaled Hydrogen

	$^3B_1$			$^1B_1$			$^1A_1$		
θ, deg	$\langle x^2 \rangle$[b]	$\langle y^2 \rangle$	$\langle z^2 \rangle$	$\langle x^2 \rangle$	$\langle y^2 \rangle$	$\langle z^2 \rangle$	$\langle x^2 \rangle$	$\langle y^2 \rangle$	$\langle z^2 \rangle$
80	1.19187	0.77641	1.17379	1.17205	0.78347	1.17373	1.32786	0.60174	1.18538
100	1.06808	0.77606	1.28348	1.05691	0.78377	1.28351	1.20812	0.61391	1.29743
120	0.94976	0.77572	1.38829	0.94472	0.78298	1.38546	1.08706	0.62334	1.39815
140	0.85477	0.77573	1.46854	0.85365	0.78108	1.46080	0.96799	0.75583	1.46881
160	0.79572	0.77610	1.51452	0.79660	0.77883	1.50101	0.82672	0.74525	1.50619

[a] Coordinate system as in Figure 1. [b] $\langle x^2 \rangle = \langle \psi | \sum_{i=1}^{8} x_i^2 | \psi \rangle / 8$.

ceptibility value characteristic of the CH_2 group. It is rather remarkable that almost all measurements indicate a value for χ between -11×10^{-6} and -12×10^{-6}. Since this experimental χ includes χ^P, we see $\chi_L < \chi$. Our result for χ_L is consistent with this inequality, but since χ^P is probably of the order of 0.5×10^{-6} our computer χ_L is probably too large. If we neglect the paramagnetic contribution to the diamagnetic susceptibility, we may estimate the diamagnetic anisotropy of the CH_2 group from the elements of $\chi_{\alpha\beta}^d$. With the coordinate system defined by Figure 1 this tensor is diagonal. If we interpolate the data in Table XV to the equilibrium angle of the $^1A_1$ state we obtain, using 5, $\chi_{xx}^d = -18.59 \times 10^{-6}$, $\chi_{yy}^d = -23.74 \times 10^{-6}$, and $\chi_{zz}^d = -16.90 \times 10^{-6}$, whereas for the $^1B_1$ state we obtain $\chi_{xx}^d = -21.46 \times 10^{-6}$, $\chi_{yy}^d = -21.94 \times 10^{-6}$, and $\chi_{zz}^d = -15.32 \times 10^{-6}$. From these values one may construct any one of the three independent components of the anisotropy tensor. These calculated values are consistent with the intuitive interpretation that the absolute magnitude of $\chi_{\alpha\alpha}$ measures the density of electrons in the plane orthogonal to the α axis. Thus we see that χ_{xx}^d and χ_{yy}^d are very different for the $^1A_1$ state (highly bent) and very similar for the $^1B_1$ state (very shallow minimum at a larger angle).

C. Quadrupole Tensor (Atomic units, ea_0^2, origin at carbon). We take as our definition

$$\Theta_{\alpha\beta} = \sum_{j=1}^{2}(3R_{j\alpha}R_{j\beta} - \delta_{\alpha\beta}R_j^2)/2 - \langle\psi|\sum_{i=1}^{8}(3r_{i\alpha}r_{i\beta} - \delta_{\alpha\beta}r_i^2)/2|\psi\rangle$$

This tensor is traceless and in C_{2v} symmetry diagonal. We need therefore consider only two of the diagonal elements and we choose Θ_{xx} and Θ_{zz}. We present in Table XVI the quadrupole moments as calculated with the VB III and MO* functions. Shown in Figure 8 is the Θ_{zz} element as calculated with VB III. Insight into the relative magnitudes of the quadrupole moments of the $^1A_1$* and $^{1,3}B_1$ states may be obtained by considering the difference

$$\Delta\Theta_{\alpha\beta} = \Theta_{\alpha\beta}(A_1) - \Theta_{\alpha\beta}(B_1)$$

For the xx element we have

$$\Delta\Theta_{xx} = -\langle A_1|\sum_{i=1}^{8}(3x_i^2 - r_i^2)/2|A_1\rangle + \langle B_1|\sum_{i=1}^{8}(3x_i^2 - r_i^2)/2|B_1\rangle$$

The average value of $\sum_{i=1}^{8} r_i^2$ is a measure of the size of the molecule and as such is not very different for states of different symmetry. We consider the sign of $\Delta\Theta_{xx}$ to be determined by the difference

$$\Delta\Theta_{xx} \sim \langle B_1|\sum_{i=1}^{8}x_i^2|B_1\rangle - \langle A_1|\sum_{i=1}^{8}x_i^2|A_1\rangle$$

which is negative. Likewise for $\Delta\Theta_{zz}$ we arrive at

$$\Delta\Theta_{zz} \sim \langle B_1|\sum_{i=1}^{8}z_i^2|B_1\rangle - \langle A_1|\sum_{i=1}^{8}z_i^2|A_1\rangle$$

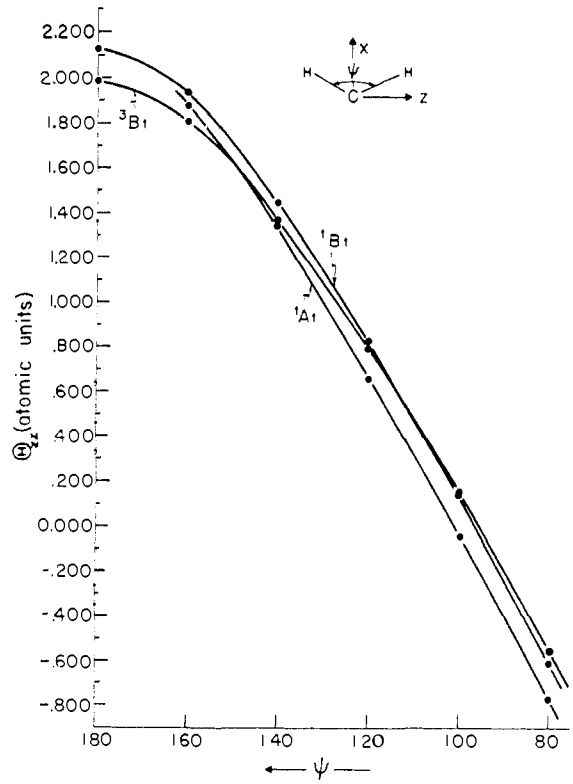

Figure 8. Θ_{zz} element of the quadrupole tensor *vs.* angle for various states of CH_2. VB—doubly occupied 1s and scaled hydrogens.

As noted in section B this difference is negative, as required.

D. Electric Field Gradient Tensor. We take as the definition of the electric field gradient tensor

$$q_{\alpha\beta}(\vec{x}) = -\langle\psi|\sum_{i=1}^{8}(3r_{i\alpha}r_{i\beta} - \delta_{\alpha\beta}r_i^2)/r_i^5|\psi\rangle + \sum_{j=1}^{3}Q_j(3R_{j\alpha}R_{j\beta} - \delta_{\alpha\beta}R_j^2/R_j^5) \quad (6)$$

where r_i is the position vector to the ith electron and R_j is the position vector to the jth nucleus, both measured from the point $\vec{x}$ as the origin, and Q_j is the change of jth nucleus. The tensor is expressed in units of e/a_0^3 (atomic units). The elements $q_{xx}(H)$, $q_{zz}(H)$, and $q_{xz}(H)$ were calculated from eq 6 using the VB III functions. From these values we calculated the components in the principal axis system. These are presented in Table XVII along with α, the angle of rotation of the principal axis system from the CH bond (see Figure 9).

The nuclear quadrupole moment Q is measured

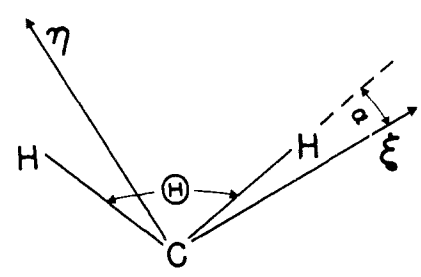

Figure 9. Principle axis system for electric field gradient tensor.

Table XVI. Quadrupole Moments of Methylene (Origin at Carbon)

	Θ_{xx} (atomic units, ea_0^2)					Θ_{zz} (atomic units, ea_0^2)				
	MO		VB[d]			MO		VB[d]		
θ, deg	$^1A_1$* [b]	$^{1,3}B_1$[c]	$^1A_1$	$^1B_1$	$^3B_1$	$^1A_1$* [b]	$^{1,3}B_1$[c]	$^1A_1$	$^1B_1$	$^3B_1$
80	−0.3342	1.398	−0.3966	1.494	1.308	−0.7741	−0.5789	−0.7705	−0.6096	−0.5591
100	−0.9884	0.7010	−1.061	0.7720	0.6537	−0.0352	0.1531	−0.0495	0.1365	0.1466
120	−1.509	0.0692	−1.610	0.1160	0.0579	0.6917	0.8403	0.6564	0.8271	0.7958
140	−1.747	−0.4895	−1.842	−0.4580	−0.4573	1.394	1.465	1.341	1.449	1.370
160	−1.414	−0.9011	−1.246	−0.8916	−0.8415	1.925	1.934	1.877	1.932	1.809
180	...	...	...	−1.063	−0.9929	...	...	...	2.126	1.986

[a] Coordinate system is defined in Figure 1. [b] This state was constructed by a variational calculation over the two determinants defined by the configurations $(1a_1)^2(2a_1)^2(1b_2)^2(3a_1)^2$ and $(1a_1)^2(2a_1)^2(1b_2)^2(1b_1)^2$. [c] These states were constructed from the configuration formed by a single excitation out of the $3a_1$ MO to the $^1b_1$ virtual orbital. [d] VB—doubly occupied 1s and scaled hydrogen.

Table XVII. Electric Field Gradient Tensor in Atomic Units[a]

	$^1A_1$			$^1B_1$			$^3B_1$		
θ, deg	α[b]	$q_{\xi\xi}$[c]	$q_{\eta\eta}$[d]	α	$q_{\xi\xi}$	$q_{\eta\eta}$	α	$q_{\xi\xi}$	$q_{\eta\eta}$
80	4° 52′	0.4836	−0.2705	6° 53′	0.4610	−0.2171	5° 31′	0.4587	−0.2179
100	2° 29′	0.4730	−0.2724	4° 11′	0.4552	−0.2203	2° 53′	0.4568	−0.2222
120	1° 16′	0.4657	−0.2722	2° 39′	0.4518	−0.2205	1° 28′	0.4562	−0.2234
140	45′	0.4575	−0.2645	1° 35′	0.4486	−0.2208	37′	0.4538	−0.2237
160	34′	0.4406	−0.2353	44′	0.4457	−0.2216	9′	0.4502	−0.2240
180	...	...	...	0°	0.4445	−0.2226	0°	0.4483	−0.2242

[a] (At proton in methylene) in principal axis system, VB—doubly occupied 1s and scaled hydrogen. Units are e/a_0^3. [b] Angle between the ξ axis and the CH bond. [c] Electric field gradient along the ξ axis of the principal axis system. [d] Electric field gradient along the η axis of the principal axis system.

Table XVIII. Average Values of $1/r$[a]

	$^3B_1$		$^1B_1$		$^1A_1$	
θ, deg	$\langle 1/r_C\rangle$[b]	$\langle 1/r_H\rangle$	$\langle 1/r_C\rangle$	$\langle 1/r_H\rangle$	$\langle 1/r_C\rangle$	$\langle 1/r_H\rangle$
80	1.97234	0.55608	1.98196	0.55383	1.95742	0.55204
100	1.96655	0.54767	0.97907	0.54701	0.95776	0.54500
120	1.96306	0.50489	1.95762	0.54092	1.95906	0.53907
140	1.96227	0.53584	1.97112	0.53552	1.96110	0.53435
160			1.96657	0.53122	1.96300	0.43120

[a] VB—doubly occupied 1s and scaled hydrogen. Units of $1/a_0$. [b] $\langle 1/r_A\rangle = \langle\psi|\sum_{i=1}^{8} 1/r_{Ai}|\psi\rangle/8$.

in units of $e \times 10^{-26}$ cm^2 and the quadrupole coupling constant (in kilocycles/second) is

$$\nu\ (\text{kc/sec}) = (e^2/a_0^3 h)q(\text{au})Q \times 10^{-29}$$

therefore $\nu = 2350.45qQ$. The most recent value for the quadrupole moment of the deuteron is 0.2796 e $\times 10^{-26}$ cm^2 and thus our expression for the deuteron coupling constant is $\nu_D = 657.3q$ (au). From the data listed in Table XVIII we interpolate the values 309, 294, and 298 kc/sec for, respectively, the $^1A_1(108°)$, $^1B_1(148°)$, and $^3B_1(138°)$ coupling constants. These correspond to the $q_{\xi\xi}$ field gradient. There are no experimental data at present.

Expectation Values of $1/r_C$ and $1/r_H$. We define

$$\langle 1/r_A\rangle = \left\langle \psi \middle| \frac{1}{8}\sum_{i=1}^{8} 1/r_{iA} \middle| \psi \right\rangle \qquad (7)$$

where r_{iA} represents the distance of electron i from nucleus A. We present in Table XVIII the values of $\langle 1/r_C\rangle$ and $\langle 1/r_H\rangle$ as calculated from our VB III function. From the data in Table XVIII we may evaluate the isotropically averaged diamagnetic contribution to the nuclear magnetic shielding constants at the proton and carbon atoms. We take as our definition

$$\sigma^d(A) = (e^2/3mc^2)\langle\psi|\sum_{i=1}^{8} 1/r_{iA}|\psi\rangle$$

where r_{iA} is defined as in eq 7. If we evaluate the integral in atomic units ($1/a_0$) we have

$$\sigma^d(A) = 1.775 \times 10^{-5}\langle\psi|\sum_{i=1}^{8} 1/r_{iA}|\psi\rangle$$

$$\sigma^d(A) = 14.20 \times 10^{-5}\langle 1/r_A\rangle$$

Interpolation of the data in Table XVII yields $\sigma^d(H)$ as 7.705×10^{-5}, 6.580×10^{-5}, and 7.615×10^{-5} for $^1A_1(108°)$, $^1B_1(148°)$, and $^3B_1(138°)$, respectively. We note that according to our previous interpretation electron promotion from the $3a_1$ to the $1b_1$ orbital we would expect the protons in the $^1A_1$ state to be more shielded than those in a B_1 state just as our numerical results indicate.

V. Background and Previous Work

A. Theoretical. Speculation as to the electronic structure of methylene dates from the 1932 work of Mulliken.[13] He reasoned that if carbon were sp^3 hybridized the HCH angle would be a little larger than the tetrahedral value, while if the atom was not

(13) R. S. Mulliken, *Phys. Rev.*, **41**, 751 (1932).

hybridized the angle would be about 90°. Therefore, the HCH angle was judged to have an intermediate value (the possibility of sp^2 or sp hybridization was not mentioned). A $^1A_1$ ground state and a first excited $^3B_1$ state were assumed. Lennard-Jones[14] in 1934 constructed a correlation diagram for the series O, NH, CH_2, and from the known atomic levels in O he deduced that the one-electron orbitals in CH_2 should decrease in stability along the sequence $1a_1$, $2a_1$, $1b_2$, $3a_1$, $1b_1$. He also concluded that the ground state should be $^1A_1$ and the first excited state $^3B_1$. This prediction was made at a time when no detailed knowledge could be obtained about the difference in stability between the $3a_1$ and $1b_1$ orbitals or its dependence on the HCH angle. Voge[15] cautioned against using only the carbon sp^3 configuration in considering the CH_2 angle. He pointed out that if one considered VB structures which included sp hybridization, the equilibrium angle would be much larger than the tetrahedral angle. Lennard-Jones and Pople[16] made a qualitative prediction that the methylene triplet was linear and that the singlet would be bent. They further noted that detailed calculation would be necessary to ascertain the ground-state multiplicity. Linnet and Poë[17] present a very interesting argument for a nonlinear triplet. They write down the determinatal wave function ψ corresponding to the ^3p state of oxygen and form the electron distribution function ψ^2. The electronic coordinates which maximize this function are sought subject to the constraint that the symmetry of the resulting electron distribution is C_{2v}. They concluded that the configuration of maximum probability was that which had (a) two electrons at the oxygen nucleus, (b) four electrons distributed in two pairs which are separated by an angle of 133.5°, and (c) two single electrons being separated by an angle of 103°. The plane of the pairs is at right angles to the plane of the single electron and the angle between a single electron and a pair is 104.5°. Linnett and Poë argue that the free carbon atom has as its configuration of maximum probability four electrons at the vertices of a tetrahedron (109.5°), while in the united atom limit the angle between electron pairs is 133.5°. Since the methylene triplet is an intermediate configuration it should have a HCH angle between 109.5 and 133.5°.

The first calculation to consider all electrons was a semiempirical attempt by Niira and Oohata.[18] They employed the VB method including those covalent states that may be constructed from the atomic configurations $k^2s^2p^2h^2$ and $k^2sp^3h^2$. This results in six determinants with carbon as s^2p^2 and seven with carbon as sp^3. They symmetrize this basic set and construct secular equations for the various singlets and triplets of CH_2. Overlap integrals are neglected, and the matrix elements of the Hamiltonian over the determinantal wave functions are approximated by (a) expressing part of each matrix element in terms of atomic valence-state energies which are obtained from spectroscopy; (b) parameterizing the interaction between the k shell of carbon and the 1s orbital of hydrogen, the parameter being evaluated from the electronic spectrum of CH. (c) The interaction energy between the two hydrogen atoms was obtained from the Morse curve for hydrogen, and (d) the remaining two electron and nuclear attraction integrals are evaluated using single-term STO's for the carbon 2s and sp orbitals. Their results were $^3B_1(140°) < {}^1B_1(\sim 120°) < {}^1A_1(\sim 110°)$ with a dissociation energy of 9.25 eV, $^3B_1$–$^1B_1$ separation of 1.5 eV, and $^1B_1$–$^1A_1$ approximately 0.6 eV.

Walsh[6] in his discussion of the geometry of AH_2 molecules suggest that in the ground state methylene is probably bent and that the multiplicity depends on the HCH angle. He expects that if the molecule is found to have a large angle the ground state is probably a triplet, whereas a small angle indicates a singlet ground state. He predicts that the allowed transition $^1A_1 \rightarrow {}^1B_1$ will be similar to the α bands of NH_2 and anticipates a large change in angle in going to the $^1B_1$ state. These predictions seem well borne out by experiment.[8]

Gallup[19] attempted to ascertain the multiplicity of the ground state by employing a Hückel-like theory. He took an atomic orbital basis consisting of carbon valence orbitals and a 1s on each hydrogen atom. The elements of the Hamiltonian were taken to have the form

$$H_{ij} = (H_{ii} + H_{jj} - 10.0)S_{ij}/2$$

where the diagonal elements H_{ii} were not given but were said to be "empirically determined atomic orbital energies for carbon and hydrogen." Slater orbitals were used to calculate the overlap integrals. The sum of the one-electron energies over the first three spatial MO's is taken as the singlet energy. To estimate the triplet energy, one promotes an electron from the highest filled to the lowest empty MO, takes the sum of the one-electron energies, and then adds −1.3 eV to this sum. The 1.3-eV is the difference between the ^3P and ^1D states of free carbon[11] and is taken as a measure of the energy increase in pairing two electrons of opposite spin. Gallup arrives at the conclusion that the triplet state is lower than the singlet for the angles he considered (100–180°). The energy difference is of course never greater than 1.3 eV.

The first *ab initio* calculation in which all integrals were evaluated was carried out by Foster and Boys.[7] They consider six STO's on the carbon atom and an 1s orbital on each hydrogen which they form into orthogonal MO's. These MO's are used to define exclusive orbitals, *i.e.*, that orthonormal set of functions which have their centroids of charge as far apart from one another as is possible. Then, for each occupied exclusive orbital they define a set oscillator orbitals composed of a linear combination of the unoccupied exclusive orbitals. These oscillator orbitals have the property that the square of the dipole moment matrix elements between them and the corresponding occupied exclusive orbital is a maximum. The variation calculation is carried out over the determinants formed from the exclusive orbitals and single and double replacements of these exclusive orbitals by their corresponding oscillator orbitals. Foster and Boys report that this leads to 128 functions for the $^3B_1$ symmetry. They

(14) J. E. Lennard-Jones, *Trans. Faraday Soc.*, **30**, 70 (1934).
(15) H. Voge, *J. Chem. Phys.*, **4**, 581 (1936).
(16) J. E. Lennard-Jones and J. A. Pople, *Discussions Faraday Soc.*, **10**, 9 (1951).
(17) J. W. Linnett and A. J. Poë, *Trans. Faraday Soc.*, **47**, 1033 (1951).
(18) K. Niira and K. Oohata, *J. Phys. Soc. Japan*, **7**, 61 (1952).
(19) G. A. Gallup, *J. Chem. Phys.*, **26**, 716 (1957).

predict the level order $^3B_1(129°) < {}^1A_1(90°) < {}^1B_1$ (132°) for all angles between 90 and 180°.

Padgett and Krauss[20] carried out the first molecular orbital SCF treatment. They used an STO basis with Slater exponents and used the Mulliken approximation for the three-center electron interaction integrals. They predict $^3B_1(120°) < {}^1A_1(90°) < {}^1B_1(130°)$ for all angles from 90 to 180°. Because of the small separation between their $^3B_1$ and $^1A_1$ states, they are reluctant to make a choice as to which is the ground state since the effect of Mulliken approximation could not be assessed.

King and Malli[21] have carried out a MO–CI on linear methylene. They consider the carbon 1s electrons as shielding the nucleus and treat the methylene as a six-electron problem. They use single exponentials for the carbon orbitals and the two hydrogen 1s functions. The atomic orbitals are combined into basis functions for the $D_{\infty h}$ group. Since there are six one-electron functions, one may form $\binom{6}{3}^2 = 400$ determinants having $S_z = 0$. Of these 400 they neglect those 20 which would place each of the six electrons in a different spatial orbital. The variation calculation is then carried out for states of definite symmetry and spin. The order of the first three states is $^3\Sigma_g^- < {}^1\Delta_g < {}^1\Sigma^+$, in accordance with Hunds rules.

Jordan and Longuet-Higgins[22] used a novel semiempirical approach in considering the electronic structure of AH_2 molecules. They write the total energy as

$$E(\lambda,\theta) = E_A(\lambda) + 2E_H(\theta,\lambda) + 2E_H$$

where λ is a measure of the 2s–2p hybridization and θ is the HCH angle. $E_A(\lambda)$ is the energy of atom A in the valence state appropriate to the molecular state under consideration, $E_{AH}(\theta,\lambda)$ is the AH bond energy, and E_H is the energy of an isolated hydrogen atom. The hybrid orbitals defined by λ do not necessarily lie along the line joining the A and H nuclei. For CH_2 $E_c(\lambda)$ is expressed in terms of the energies of the various spectroscopic levels of carbon; $E_{CH}(\theta,\lambda)$ is written as the sum of three exchange integrals $\langle 2s(1)h(2)|1/r_{12}|h(1)2s(2)\rangle$, $\langle 2p(1)h(2)|1/r_{12}|h(1)2p(2)\rangle$, and $\langle 2s(1)h(2)|1/r_{12}|h(1)2p(1)\rangle$, which are not calculated but are given values consistent with the observed energy of formation of CH_4, CH_3, and CH (their energy of formation expression assumes perfect pairing). Minimization with respect to λ at each θ results in $^3B_1(180°) < {}^1A_1(105.5°) < {}^1B_1(180°)$. They calculate an energy of formation of $-64{,}320$ cm^{-1} and

$$^3B_1(180°) \leftrightarrow {}^1A_1(105.5°) = 0.450 \text{ eV}$$

$$^3B_1(180°) \leftrightarrow {}^1A_1(180°) = 0.981 \text{ eV}$$

$$^1A_1(105.5°) \leftrightarrow {}^1B_1(180°) = 0.981 \text{ eV} - 0.450 \text{ eV} = 0.531 \text{ eV}$$

$$^1A_1(105.5°) \leftrightarrow {}^1B_1(105.5°) \cong 1.8 \text{ eV}$$

Using an approximate equation proposed by Mulliken[23] for the heat of formation of a molecular system, Pedley[24] calculated that the triplet state of CH_2 is more stable than the singlet. He hybridized the 2s and 2p orbitals of carbon into four linearly independent functions. The hybridization depends on the HCH angle being sp in the linear molecule and passing through sp^2 and sp^3 as the angle is varied. The assumption of perfect pairing is maintained for all angles, and one always has two nonbonding electrons in different spatial orbitals. The difference between the singlet and triplet states, in this theory, is due to a single exchange integral between this nonbonding orbital. However, this integral was not calculated but was estimated from the atomic spectrum of free carbon.

A most interesting attempt has been a semiempirical approach by Ellison.[25] He uses an atomic basis consisting of carbon 1s, 2s, $2p_x$, $2p_y$, $2p_z$, and two hydrogen 1s functions. The carbon 2s, $2p_x$, $2p_y$ orbitals are hybridized such that one orbital lies along the C_2 axis, while the other two point directly toward the hydrogen atoms. The $2p_z$ orbital has a node in the molecular plane (b_1 sym). He writes determinantal wave functions for the singlet and triplet B_1 states as well as the first two states of $^1A_1$ symmetry. The energy expression for a given structure is reduced to the form

$$E_i = E_C^* + E_{H_2}^* + \tilde{J} + \tilde{X} - \tilde{Y}$$

where E_C^* and $E_{H_2}^*$ are the valence-state energies of the carbon and hydrogen atoms, respectively. $\tilde{J}$ is proportional to the Coulomb energy, $\tilde{X}$ is proportional to the exchange energy which arises from single and multiple permutations of covalently bonded electrons, and $\tilde{Y}$ is proportional to the exchange energy involving single permutations of nonbonded electrons. The energy expression contains three undetermined parameters which are fixed by calibrating the theory with the heat of atomization of the 2π, $^2\Delta$ states of CH and the ground state of CH_4. The predicted order of the first four states is $^3B_1(180°) < {}^1A_1(100°) < {}^1B_1(180°) < {}^1A_1(180°)$. The estimated vertical transition energies are

$$^1A_1(100°) \leftrightarrow {}^1B_1(100°) = 4.35 \text{ eV}$$

$$^3B_1(180°) \leftrightarrow {}^1A_1(180°) = 0.92 \text{ eV} \; (\equiv {}^3B_1(180°) \leftrightarrow {}^1B_1(180°))$$

$$^3B_1(180°) \leftrightarrow {}^1A_1(100°) = 0.62 \text{ eV}$$

Coulson and Stamper[26] have studied the Rydberg levels in CH_2 which are associated with the carbon 3d orbital. They restricted the molecule to the linear configuration and confirmed Herzberg's[7] assignment of the vacuum ultraviolet bands ($^3\Sigma_g^- \rightarrow {}^3\Sigma_u^-$ and $^3\Sigma_g^- \rightarrow {}^3\Pi_u$) as being transitions to essentially Rydberg levels involving the carbon 3d electron.

Dixon[27] has carried out a rather extensive study of the $^3B_1$, $^1A_1$, and $^1B_1$ states of methylene as a function of the H–C–H angle. He employed the basis functions and integrals used by Padgett and Krauss.[20] Both the VB and ICC[28] methods were employed. His results are, for the (limited) VB

(20) A. Padgett and M. Krauss, *J. Chem. Phys.*, **32**, 189 (1960).
(21) G. W. King and G. L. Malli, *Can. J. Chem.*, **39**, 1652 (1961).
(22) P. C. H. Jordan and H. C. Longuet-Higgins, *Mol. Phys.*, **5**, 121 (1962).
(23) R. S. Mulliken, *J. Phys. Chem.*, **56**, 295 (1952).
(24) J. B. Pedley, *Trans. Faraday Soc.*, **58**, 23 (1962).
(25) F. O. Ellison, *J. Chem. Phys.*, **36**, 3107 (1962).
(26) C. A. Coulson and J. G. Stamper, *Mol. Phys.*, **6**, 609 (1963).
(27) R. N. Dixon, *ibid.*, **8**, 201 (1964).
(28) W. Moffitt, *Proc. Roy. Soc.* (London), **A210**, 245 (1951); A. C. Hurley, *ibid.*, **A248**, 119 (1958); **A249**, 402 (1959).

$$^3B_1(180°) < {}^1A_1(\sim 100°) < {}^1B_1(\sim 150°)$$

while for the ICC he obtains

$$^3B_1(180°) < {}^1A_1(105°) < {}^1B_1(180°)$$

Recently, Hoffmann, Zeiss, and Van Dine[29] applied the extended Hückel method to a series of methylenes among which was the parent compound methylene. The criterion for assigning the ground-state multiplicity was the same as Gallup's. The triplet was taken as the ground state if the sum of the one-electron energies of the lowest singly excited configuration was not greater than the comparable sum for the lowest doubly occupied configuration by more than 1.5 eV (recall Gallup used 1.3 eV). A triplet state with a very shallow minimum at about 155° and a highly bent singlet with an angle around 115° are predicted.

Today's level of electronic structure theory understanding permits us to state in summary that only the calculations of Foster and Boys[7] and the present work yield sufficient quantitative information to provide a broadly significant contribution to the structure and properties of CH_2.

B. Experimental. Herzberg[7] has observed the spectrum of methylene in a flash photolysis experiment using diazomethane, CH_2N_2, as the parent compound. Methylene seems to be formed in an excited singlet state which by collisional deactivation with excess N_2 decays to the lowest singlet state, $^1A_1$. This state may either absorb radiation and make a transition to the $^1B_1$ state or decay by collisional deactivation to the $^3B_1$ ground state. That $^3B_1$ is probably the ground state is deduced by the influence of the inert gas pressure on the intensity of the absorption spectrum. The red bands of CH_2, between 1.3 and 2.25 eV, are assigned to $^1A_1(103°) \rightarrow {}^1B_1(\sim 180°)$. The transition in the vacuum ultraviolet, around 8.75 eV, is assigned to $^3B_1$(large angle $\sim 180°$) $\rightarrow {}^3A_1(\sim 180°)$. This transition has been identified as the first in a Rydberg series leading to the ionization potential of 10.396 eV and probably involves carbon $3d_{\pi g}$ electrons.[26]

The summary of experimental information above and that given in section III.C is limited to that most pertinent for the comparison and verification of our theoretical calculations. A more extensive review of CH_2 spectroscopy along with an excellent review of CH_2 insertion and addition reactions has been written by Gaspar and Hammond.[2] Their thorough experimental review forms a complement to our theoretical review section. In their own review of theoretical developments they conclude with a note of concern, "A thought-provoking lesson is told by the tendency of theoretical conclusions to become more guarded as the work becomes more quantitative and sophisticated." We certainly wish the present results to be regarded with conservatism and there is certainly room for a greatly improved theoretical treatment, but it is satisfying that for CH_2 theoretical and experimental evidence are at a roughly comparable level of conclusiveness and the relatively small differences now existing may be regarded as a genuine uncertainty in our present knowledge. It is also important to have provided a number of quantitative theoretical predictions for energy level separations and several other properties that have not as yet been measured.

(29) R. Hoffman, G. D. Zeiss, and G. W. Van Dine, *J. Am. Chem. Soc.*, **90**, 1485 (1968).

VI. Summary and Conclusions

In this paper we have constructed *ab initio* valence-bond and molecular orbital wave functions for the $^3B_1$, $^1A_1$, and $^1B_1$ states of methylene as a function of the HCH angle with R(C—H) = 2.00 bohrs. These wave functions are the most accurate ever computed for a group of states in a polyatomic molecule, and we have used them to predict and explain the chemistry and spectroscopy of gas-phase CH_2.

Our calculations led to a state ordering and geometry (VB III, see Figure 5) of $^3B_1(138°) < {}^1A_1(108°) < {}^1B_1(148°)$, which is to be compared with Herzberg's spectroscopic conclusions: $^3B_1(\sim 160\text{–}180°) < {}^1A_1(103°) < {}^1B_1(\sim 140°)$.

Figure 3 compares total energies and state ordering *vs.* angle for our three valence-bond wave functions, and it is apparent that the calculations of lowest energy (VB III) give the best agreement with spectroscopic results. This is as it should be and the summary presented in this section deals almost entirely with VB III. However, for VB I we purposely set up a wave function to prevent s–p hybridization by requiring double occupancy of the 2s orbital, and this wave function provides a quantitative answer to a long standing debate. Figure 3 shows directly that if there is no s–p hybridization a singlet ground state ($^1A_1$) is obtained with an equilibrium bond angle very near to 90°. An electron in $2p_x$ pairs with one hydrogen and a $2p_z$ electron pairs with the other hydrogen, but this results in a high-energy (compared to the $^3B_1$ of VB III) state because denial of s–p mixing keeps the orbitals from taking optimal advantage of the positive molecular framework potential. The ionization potential of hydrogen is almost midway between those of the carbon 2s and 2p, and a strong mixing of these three orbitals minimizes the energy. A linear configuration allows two unmixed orbitals (p_x, p_y) which can be singly occupied and have parallel spins, thus lowering the energy. For bent configurations the $2p_x$ mixes with the 2s and hydrogens. While this lowers the energy, favoring bending ($3a_1$ orbital, see section II.D), the orbital must be only singly occupied to retain the energy advantage of parallel spin. The other singly occupied orbital is the p_y, and since this is perpendicular to the molecular plane it is almost entirely independent of angle. In the linear configuration the $3a_1$ is $2p_x$ and degenerate with $2p_y$. For smaller angles it varies slowly, thus maintaining a roughly constant compromise between the spin-pairing energy and $3a_1$ orbital energy lowering due to $2s\text{–}2p_x$ hybridization. The result is a flat potential energy curve for the $^3B_1$ state. This analysis also provides a hypothesis on the shape and states of SiH_2. Although the difference in ionization potential between the valence shell s and p electrons is almost the same for carbon and silicon, the ionization potential for hydrogen is very close to the Si 3s and far from the Si 3p. Thus the orbital mixing is primarily 3s–hydrogen with the p_x, p_y, and p_z retaining their free atom condition and leading to a singlet $^1A_1$ ground state at an angle of 90°.

The $^3B_1\text{–}{}^1A_1$ excitation energy (not known experi-

mentally) is computed to be 1.77–2.10 eV (41–48.5 kcal/mole). Most of the energy difference between these two states is the spin-pairing energy in the carbon atom represented by the ^3P–^1D energy separation. This energy is spectroscopically determined to be 1.26 eV (29.1 kcal) while a carbon atom computation with our atomic basis orbitals yields 1.58 3 eV (36.4 kcal), thus justifying a lower bound estimate of 1.77 − 0.32 = 1.45 eV (33.4 kcal) for the $^3B_1$–$^1A_1$ separation. It is apparent from these numbers that molecular formation increases the energy separation of the ground and first excited state. Unfortunately, even this lower bound seems to be 1.5–3 times greater than values often quoted informally by organic chemists. The principal suggestion that can be offered to them on this matter is to favor those rationalizations of reaction mechanisms corresponding to a large energy separation (of course, it is also conceivable that in all of carbene chemistry one never actually obtains the free CH_2 species).

Heats of atomization for the $^3B_1$, $^1A_1$, and $^1B_1$ states are respectively 6.36 eV (147 kcal; experimental value $\cong$ 8.5 eV = 196 kcal), 6.58 eV (152 kcal), and 5.74 eV (133 kcal). See section III.B for the reactions defining these energies.

The theoretical prediction of transition energies and oscillator strengths falls into two categories: triplets and singlets. Excited triplets seem likely to be Rydberg states and this coupled with the flatness of the $^3B_1$ curve render meaningful predictions impossible with our present wave functions. By contrast our singlet–singlet transition ($^1A_1 \rightarrow {}^1B_1$) energy, 1.52 eV, agrees well with the experimental values (red bands at 1.51, 1.70, and 1.90 eV). This gives us confidence that our prediction of the experimentally unknown oscillator strengths will be quantitatively meaningful (see Table XIII). The successful prediction of the $^1A_1 \rightarrow {}^1B_1$ transition energy also adds credence to the energy we obtain for the $^3B_1$–$^1A_1$ separation.

The dipole moments of the $^{1,3}B_1$ and $^1A_1$ states are displayed in Figure 6. For the $^3B_1$ state (flat potential energy curve) the probable effective equilibrium value is approximately 0.15–0.25 ea_0 (0.38–0.635 D), and for the $^1A_1$ state (relatively sharp minimum) it is approximately 0.85 ea_0 (2.16 D). Experience with quantum mechanical calculations on many other systems indicates that these values are 30–40% too high. We might expect the $^1A_1$ to have about the same dipole moment as that of water. In any event, the ratio of the dipole moments of about 1:4 is expected to be accurate. The fact that the $^1A_1$ state dipole moment is always greater than that for the $^3B_1$ state is quantitatively described in detail on a molecular orbital basis in section IV.A. In a crude qualitative way this is reasonable simply because a singlet pair of electrons will tend to reside together in a backside orbital or carbon (away from the hydrogens) while the triplet pair of electrons will be split between the backside orbital and an average position nearer the carbon center. The electron-donating and -accepting properties of these electrons is of course governed by what species reacts with the CH_2, and an important aspect of this reaction will be the spin coupling problem. However, if we put aside these questions and only consider the charge distribution in methylene, the dipole moment ratio indicates that one would crudely expect the $^1A_1$ state to possess a donor–acceptor capability four times that of the $^3B_1$ ground state.

The diamagnetic susceptibility is a quantity of fundamental importance to organic chemistry and many indirect measurements (on homologous series) have been made to ascertain a susceptibility value for CH_2. These measurements together with an estimate of the small ($\sim$4%) paramagnetic term lead to a value for the predominate Larmor term ($\chi_L = -6.338 \times 10^{-6} \langle r^2 \rangle$) of approximately -12×10^{-6} erg/(G^2 mole). Computations based on our best valence-bond wave functions give $\chi_L = -19.75 \times 10^{-6}$ for the $^1A_1$ state and -19.57×10^{-6} for the $^1B_1$ state. Typical of the kind of detailed description obtainable from analysis of the wave function is the change in the second moment of the charge distribution, $\langle r^2 \rangle = \langle x^2 \rangle + \langle y^2 \rangle + \langle z^2 \rangle$, resulting from the promotion $A_1 \rightarrow B_1$. We find a decrease in the electron density along the x axis (rotation axis) and thus a decrease in $\langle x^2 \rangle$, an increase in electron density along the y axis (perpendicular to plane of molecule) and thus an increase in $\langle y^2 \rangle$, and a decrease in electron density along the z axis and thus a decrease in $\langle z^2 \rangle$. Further details of the charge distribution in the B_1 and A_1 states comes from our diamagnetic anisotropy calculations. For example, a measure of charge density asymmetry between the molecular plane and the plane perpendicular to the twofold rotation axis is $\chi_{yy}^d/\chi_{zz}^d \cong 1$ for the B_1 and 1.3 for the A_1 state.

Expectation values have been obtained for the quadrupole tensor (Table XVI, Figure 8), electric field gradient tensor (Table XVII), and $1/r_C$, $1/r_H$ (Table XVIII). These values represent *a priori* predictions since there are no existing experimental values, and detailed discussion of the charge distribution implied by these quantities along with a rationalization of the magnitudes computed is given in sections IV.C, D, and E. As a byproduct we find the deuterium quadrupole coupling constants for CD_2 to be 309, 294, and 298 Kc/sec for the $^1A_1(108°)$, $^1B_1(148°)$, and $^3B_1(138°)$, respectively. The diamagnetic contribution to the nuclear magnetic shielding constant of the protons (isotropically averaged, $\sigma^d(H) = 14.20 \times 10^{-5}\langle 1/r_H \rangle$) is 7.70×10^{-5}, 7.58×10^{-5}, 7.61×10^{-5} for $^1A_1(108°)$, $^1B_1(148°)$, and $^3B_1(138°)$, respectively.